

RESEARCH ARTICLE

Sp8 plays a supplementary role to Pax6 in establishing the pMN/p3 domain boundary in the spinal cord

Xiaosu Li^{1,*}, Zhidong Liu¹, Mengsheng Qiu^{2,3} and Zhengang Yang^{1,*}

ABSTRACT

Progenitor cells are segregated into multiple domains along the dorsoventral axis of the vertebrate neural tube, and each progenitor domain generates particular types of neurons. Selective cross-repressive interactions between pairs of class I and class II transcription factors play important roles in patterning neural progenitors into domains with clear boundaries. Here, we provide evidence that the zinc-finger protein Sp8 plays a supplementary role to Pax6 in establishing the pMN/p3 domain boundary through mutually repressive interactions with the class II protein Nkx2-2. The ventral limit of Sp8 expression is complementary to the dorsal limit of Nkx2-2 expression at the pMN/p3 boundary. Sp8 and Nkx2-2 exert cross-repressive interactions, and changing the expression of Sp8 and Nkx2-2 is coupled with pMN and p3 progenitor fate conversion. Sp8 exerts its neural patterning activities by acting as a transcriptional activator. The expression of a repressive form of Sp8 results in the selective inhibition of motor neuron generation and the ectopic induction of Nkx2-2 expression. Sp8 expression is positively regulated by, but not completely dependent on, Pax6. Furthermore, whereas loss of Pax6 function alone results in disruption of the pMN/p3 domain boundary only in the rostral levels of the spinal cord, loss of both Sp8 and Pax6 functions results in disruption of the pMN/p3 domain boundary along the whole rostrocaudal axis of the spinal cord. We conclude that Sp8 plays a supplementary role to Pax6 in specifying the pMN over p3 progenitor fate through cross-repressive interactions with Nkx2-2.

KEY WORDS: Sp8, Pax6, Nkx2-2, Ventral patterning, Motor neuron, Chick, Mouse

INTRODUCTION

An early and fundamental step of neural development is the generation of distinct classes of neurons in appropriate numbers and precise locations. Distinct types of neurons derive either from a common population of multipotent progenitor cells (Marquardt and Gruss, 2002; Pearson and Doe, 2004; Shen et al., 2006) or from different progenitors. In the latter case, different types of progenitors are always segregated into spatially distinct populations (Flames et al., 2007; Alaynick et al., 2011). Within the ventral spinal cord, five neuronal progenitor domains (p3, pMN, p2, p1 and p0) along the dorsoventral axis have been identified based on the expression of homeodomain/basic helix-loop-helix transcription factors (Liem

et al., 2000; Lee and Pfaff, 2001). The spatially specific expression of these transcription factors is largely controlled by graded sonic hedgehog (Shh) signaling. Shh is secreted from the notochord and floor plate and forms a ventral-to-dorsal gradient (Marti et al., 1995; Chamberlain et al., 2008; Dossaud et al., 2008). Graded Shh signaling induces class II and represses class I transcription factor expression at different thresholds – an effect that is correlated with the position-specific expression of a particular gene. The transcription factor expression profile specifies the identity of the progenitor population within an individual domain; more ventral identities are specified in regions with higher levels of Shh signaling (Ericson et al., 1997a,b; Briscoe and Ericson, 1999).

Differences in Gli binding affinity for distinct sites in the cis-regulatory modules of class II genes and the transcriptional regulatory activity state of Gli proteins both play important roles in determining threshold-level responses to Shh (Jacob and Briscoe, 2003; Stamatakis et al., 2005; Balaskas et al., 2012; Peterson et al., 2012). Selective cross-repressive interactions between pairs of class I and class II transcription factors assist in converting the continuous Shh gradient into sharp domain boundaries. Four pairs of cross-repressive transcriptional factors delineate the four ventral domain boundaries between the five neuronal progenitor domains. The two ventralmost neuronal progenitor domains, p3 and pMN, generate V3 interneurons and motor neurons (MNs), respectively, and they are distinguished and specified by expression of the transcription factors Nkx2-2 and Olig2 (Briscoe et al., 1999; Mizuguchi et al., 2001; Novitsch et al., 2001; Lu et al., 2002; Zhou and Anderson, 2002).

Recent fate-mapping studies based on the Cre-loxP strategy indicated that the Nkx2-2 and Olig2 cell lineages may share a common origin (Wu et al., 2006; Dossaud et al., 2007, 2010; Holz et al., 2010; Chen et al., 2011; Wang et al., 2011), a result that is supported by the analysis of the temporal expression profile of several transcription factors (Jeong and McMahon, 2005; Lek et al., 2010). It is therefore important to understand how the Olig2/Nkx2-2 double-positive (Olig2⁺/Nkx2-2⁺) cells diversify into Olig2⁺ pMN progenitors and Nkx2-2⁺ p3 progenitors. Previous studies have suggested that the distinction in identity of the pMN and p3 progenitor domains depends on cross-repressive interactions between Pax6 and Nkx2-2/Nkx2-9 (Ericson et al., 1997b; Briscoe et al., 1999, 2000). However, without Pax6 functions, the pMN and p3 domains are specified normally at the caudal levels of the spinal cord. Thus, Pax6 might not be the only factor that antagonizes the function of Nkx2-2 to establish the pMN/p3 domain boundary.

RESULTS

Sp8 is expressed in dP5-pMN progenitors and in a subset of postmitotic ventral neurons in the spinal cord

Previous studies in mice, chicken and zebrafish have detected Sp8 transcripts in the spinal cord during embryogenesis. Neural Sp8 mRNA expression is first detected in the forming neural tube and

¹Institutes of Brain Science and State Key Laboratory of Medical Neurobiology, Fudan University, Shanghai 200032, China. ²Institute of Developmental and Regenerative Biology, Zhejiang Key Laboratory of Organ Development and Regeneration, Hangzhou Normal University, Hangzhou 310036, China.

³Department of Anatomical Sciences and Neurobiology, School of Medicine, University of Louisville, Louisville, KY40392, USA.

*Authors for correspondence (072023029@fudan.edu.cn; yangz@fudan.edu.cn)

subsequently in the ventral spinal cord (Bell et al., 2003; Treichel et al., 2003; Kawakami et al., 2004). To analyze the expression pattern of Sp8 in detail, we performed immunohistochemistry in mouse spinal cord sections between E8.0 and E12.5 (Fig. 1; supplementary material Fig. S1). In E8.0 neural plate, whereas Pax6 was only detected at rostral levels, Sp8 was detected in nearly all cells at both rostral and caudal levels (supplementary material Fig. S1A,B). In the ventral midline, Sp8 was detected at E8.0 but gradually downregulated at E8.5 (supplementary material Fig. S1C–F). By E9.5, Sp8 was only detected in the ventral and intermediate spinal cord (neural tube) (supplementary material Fig. S1G; Fig. 1A). In E10.5 spinal cord, Sp8 expression shared the same ventral limit as Olig2 and complemented the dorsal limit of Nkx2-2 expression, indicating that the ventral limit of Sp8 expression is located at the p3/pMN boundary (Fig. 1B,D,E). Consistent with this observation, the ventral limit of Sp8 expression was always separated from the p3/FP boundary, which is marked by the dorsal limit of Shh/FoxA2 expression (Fig. 1F). We also defined the dorsal limit of Sp8 expression. Sp8 was expressed by the ventralmost dorsal progenitors, as revealed by co-labeling for Pax7 and Ascl1 in the dorsal spinal cord. Only a small portion of the Ascl1-expressing domain overlapped with the dorsal Sp8 expression domain, indicating that the dorsal limit of Sp8 expression is most likely the dP5 domain (Fig. 1G,H).

We also observed a significant number of Sp8⁺ cells scattered in the ventral spinal cord outside of the ventricular zone (VZ) at E12.0–12.5 (Fig. 1C). These Sp8⁺ cells migrated in a ventrolateral direction, which resembles the migration patterns of V0, V1, V3 interneurons and MNs. Some Sp8⁺ cells were distributed among MNs. MNs segregate into discrete columns, and each column innervates a different peripheral domain (Dasen et al., 2008; Roussou et al., 2008). Within the medial motor column (MMC), the majority of Sp8⁺ cells expressed the MN lineage genes *Lhx3*, *Hb9* (*Mnx1*) and *Isl1*. However, within the lateral motor column (LMC), the hypaxial motor column (HMC) and the preganglionic motor column (PGC), Sp8⁺ cells did not express any of these MN lineage genes (supplementary material Fig. S2D–I). These results suggest that

Sp8 expression is extinguished in the majority of the postmitotic MNs, with the exception of a subset of MMC MNs. We also observed that a subset of Hb9[−]/Isl1[−]/Lhx3⁺/Sp8⁺ cells was located dorsomedially to the MNs, suggesting a V2 interneuron identity (supplementary material Fig. S2B,E,F,H,I). A subset of Sp8⁺ cells distributed within the LMC, the HMC and the PGC expressed neither Lhx3 nor Gata3 but expressed the V1 interneuron marker En1 (supplementary material Fig. S2C). At this stage, the pMN progenitor domain begins to generate oligodendrocytes (Lu et al., 2000, 2002; Zhou et al., 2000, 2001; Zhou and Anderson, 2002; Li et al., 2011a). Sp8 was expressed in Olig2⁺ cells within the VZ but not in those outside of the VZ, suggesting that Sp8 expression is maintained in the Olig2⁺ progenitor cells but is downregulated in differentiated oligodendrocytes (supplementary material Fig. S2A).

Taken together, these results indicated that Sp8 is expressed in dP5–pMN progenitors and in a subset of postmitotic ventral neurons, including a subpopulation of MMC MNs, V2 and V1 interneurons.

Mutual repression of Sp8 and Nkx2-2 expression at the p3/pMN domain boundary

In chick embryos, the expression patterns of Sp8 and Nkx2-2 are similar to those of mouse embryos (Fig. 3A). Nkx2-2 and Sp8 share a common expression boundary but are detected in distinct domains, raising the possibility that these two factors regulate each other's expression and participate in the patterning of the ventral spinal cord. To address this possibility, we misexpressed Sp8 or Nkx2-2 by *in ovo* electroporation. Following electroporation with an Sp8-expressing vector, Sp8 expression was detected in all of the transfected cells that were labeled by GFP (Fig. 2A). We observed that 95.5±5.7% of GFP⁺ cells in the p3 domain lacked Nkx2-2 expression, whereas the expression of Nkx2-2 was retained in the neighboring untransfected p3 domain cells (Fig. 2B,G). Following electroporation with the empty control vector cUXIE, the expression of GFP alone did not change the Nkx2-2 expression patterns (Fig. 2C,G). These results suggest that Sp8 cell-autonomously

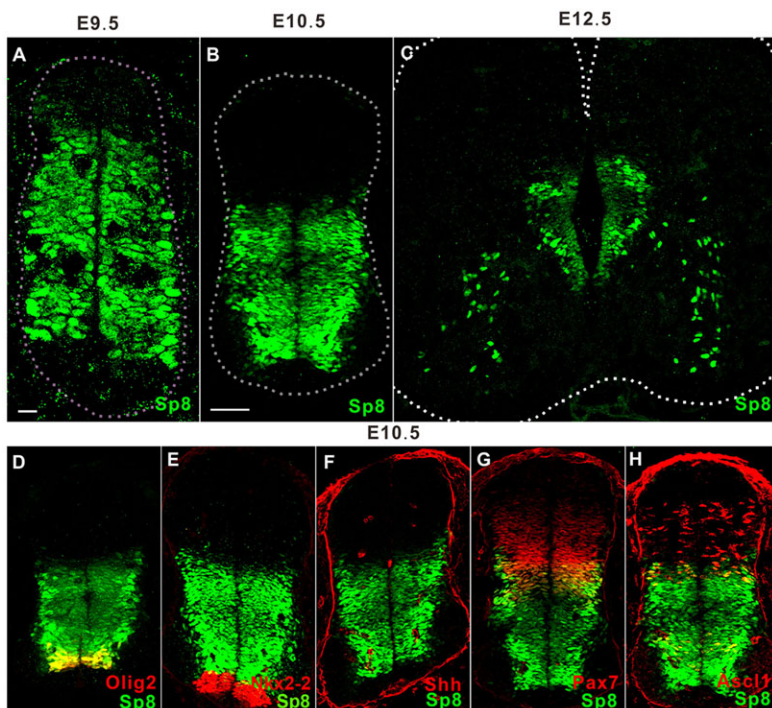


Fig. 1. Sp8 expression pattern in the developing mouse spinal cord. (A–C) Sp8 expression in transverse sections of the ventral neural tube at E9.5 (A), E10.5 (B) and E12.5 (C). (D–H) Sections from E10.5 mice showing Sp8 expression in progenitors located between the dP5 and the pMN domain. The ventralmost Sp8⁺ cells were co-labeled with Olig2, which marked the pMN domain, and all Olig2⁺ pMN progenitors expressed Sp8 (D). The ventral limit of Sp8 expression was complementary to the dorsal limit of Nkx2-2 expression at the p3/pMN boundary (E). Sp8 expression was separated from the Shh-expressing cells (F). Sp8 was expressed by the ventralmost dorsal progenitors, including dP6 and dP5 (G,H). Scale bars: 10 μm in A; 50 μm in B–H.

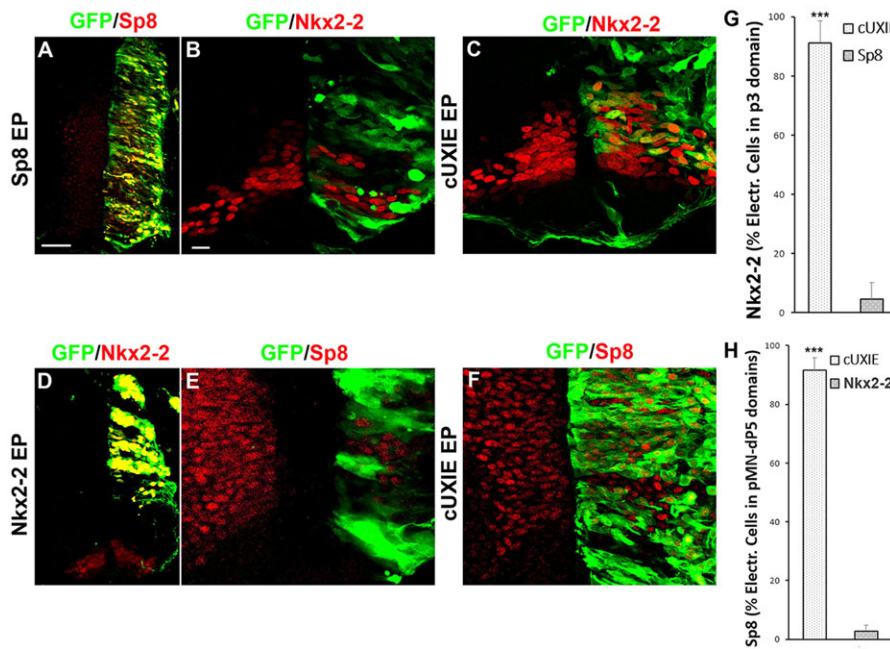


Fig. 2. Sp8 and Nkx2-2 are mutually repressive.

(A) Following the misexpression of Sp8 in chick embryos by *in ovo* electroporation (EP), Sp8 expression was detected in nearly all GFP⁺ cells. (B) Following the ventral misexpression of Sp8 in chick embryos, GFP⁺ cells in the p3 domain lacked Nkx2-2 expression. (C,F) Expression of GFP alone by electroporation of the control vector (cUXIE) did not change the expression patterns of Nkx2-2 (C) or Sp8 (F). (D) Following misexpression of Nkx2-2 in chick embryos by *in ovo* electroporation, Nkx2-2 expression was detected in nearly all GFP⁺ cells. (E) Nkx2-2 misexpression dorsal to the p3 domain resulted in the repression of Sp8 expression. (G) Quantification of the percentage of electroporated cells in the p3 domain that express Nkx2-2 after electroporation of Sp8 or cUXIE. (H) Quantification of the percentage of electroporated cells in the pMN-dPS domain that expressed Sp8 after electroporation of Nkx2-2 or cUXIE. Error bars indicate s.e.m.; *n*=3 chickens per group; ****P*<0.001 (Student's *t*-test). Scale bars: 10 μm in A for A,D; 50 μm in B for B,C,E,F.

represses Nkx2-2 expression and that the expression of Sp8 contributes to defining the dorsal limits of Nkx2-2 expression.

To examine whether Nkx2-2 normally limits the ventral boundary of Sp8 expression, we misexpressed Nkx2-2 in regions dorsal to the p3 domain (Fig. 2D). We observed that 97.3±1.9% of the cells that ectopically expressed Nkx2-2 lacked Sp8 expression (Fig. 2E,F,H), indicating that Nkx2-2 represses Sp8 expression. These results provide evidence for a mutually repressive interaction between Sp8 and Nkx2-2 at the pMN/p3 boundary.

Nkx2-2 is a class II gene that is induced by Shh signaling. To determine whether Sp8 expression is regulated by Shh signaling, we

analyzed the expression pattern of Sp8 in *Shh* mutant mouse embryos. Sp8 was expressed in the VZ of the ventral midline at the brachial level of E10.5 *Shh* mutants, similar to the expression patterns of the class I proteins Dbx1 and Dbx2 (supplementary material Fig. S3A) (Pierani et al., 1999). At the thoracic level, Sp8 expression was only detected in the subventricular zone (SVZ) but not in the VZ, and Sp8⁺ cells formed a crescent across the ventral midline (supplementary material Fig. S3B). Since MNs and V2 interneurons are almost absent from *Shh* mutants (Litington and Chiang, 2000; Persson et al., 2002), these cells are likely to be V1 interneurons. Nearly all of the Sp8⁺ cells in the VZ expressed Pax7

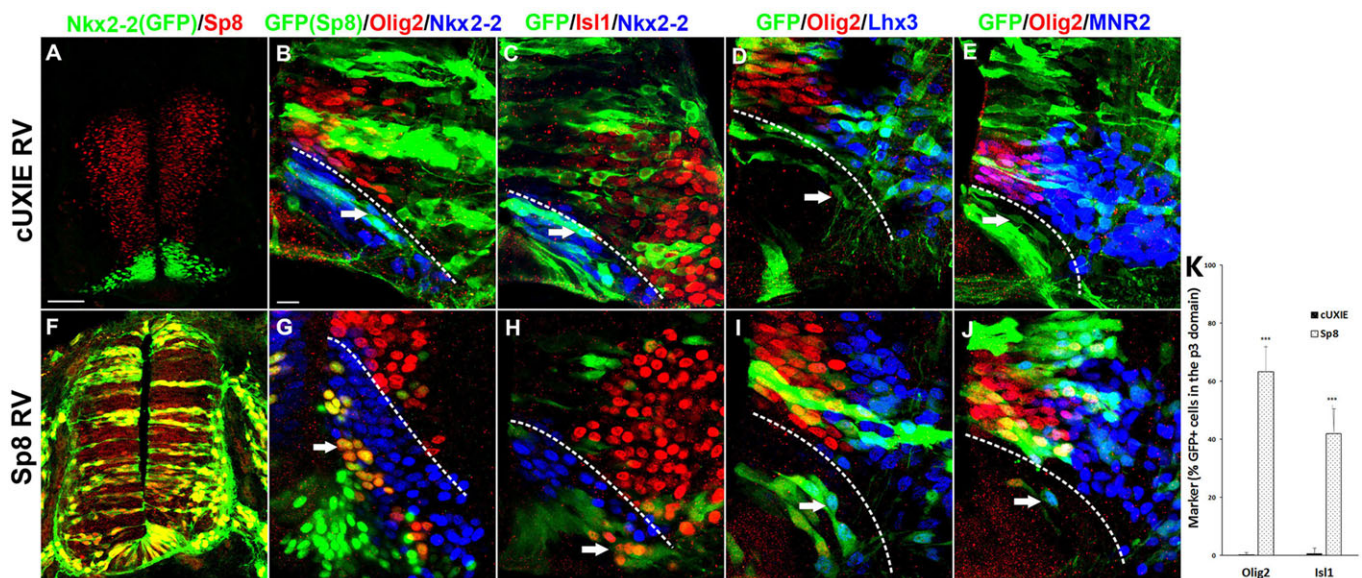


Fig. 3. Sp8 misexpression using a retrovirus directs MN generation within the p3 domain. (A) In chick embryos, the ventral limit of Sp8 expression was complementary to the dorsal limit of Nkx2-2 expression at the p3/pMN boundary. (B-E) In the chick embryos injected with control retrovirus (cUXIE RV), GFP expression alone did not change the expression patterns of the MN lineage genes *Olig2* (B), *Is11* (C), *Lhx3* (D) or *MNR2* (E). These genes were always expressed in cells located dorsal to Nkx2-2-expressing p3 progenitors. (F) Sp8 expression was detected in all of the retrovirally labeled GFP⁺ cells following injection of Sp8-expressing retrovirus. (G-J) Sp8 misexpression using retrovirus induced ectopic expression of *Olig2* (G), *Is11* (H), *Lhx3* (I) and *MNR2* (J) within the p3 domain. (B-E,G-J) The dashed lines indicate the pMN/p3 domain boundary; arrows indicate transgenic cells in the p3 domain. (K) Quantification of the above experiments. Error bars indicate s.e.m.; *n*=3 chickens per group; ****P*<0.001 (Student's *t*-test). Scale bars: 50 μm in A for A,F; 10 μm in B for B-E,G-J.

at the brachial level, whereas only a small number of $Sp8^{+}$ cells in the SVZ expressed Pax7 (supplementary material Fig. S3A,B). $Sp8$ expression extended more ventrally in the *Shh* mutant spinal cord, indicating that it is normally repressed by *Shh* signaling. Thus, we conclude that *Sp8* and *Nkx2-2* are an opposing pair of class I and class II genes that mutually repress each other's expression at the p3/pMN domain boundary.

Sp8 misexpression in the p3 domain converts the presumptive p3 progenitors into pMN progenitors

It has been conclusively demonstrated that *Nkx2-2* expression is able to direct V3 interneuron generation throughout the dorsoventral axis of neural tube (Briscoe et al., 1999, 2000), it is unclear whether the repressive effect of $Sp8$ on *Nkx2-2* expression is correlated with the specification of pMN over p3 progenitor fate. We therefore examined the expression patterns of MN lineage genes after retroviral $Sp8$ overexpression.

Following retroviral $Sp8$ overexpression, $65.3 \pm 8.5\%$ of the GFP^{+} transgenic cells within the p3 domain expressed *Olig2*, and the majority of these ectopic $Olig2^{+}$ cells lacked *Nkx2-2* expression (Fig. 3F,G,K). Moreover, a subset of more laterally positioned GFP^{+} cells expressed *Lhx3*, *Isl1* and *MNR2* within the p3 domain, mirroring the normal expression pattern of differentiating MNs (Fig. 3H–K). Ectopic pMN progenitors within the p3 domain were not observed in embryos that were infected with the control retrovirus that only expressed *GFP* (Fig. 3A–E). These results demonstrate that the ectopic $Olig2^{+}$ cells in the p3 domain that were observed following $Sp8$ misexpression acquired definitive characteristics of pMN progenitors. Whereas *Nkx2-2* misexpression directs V3 interneuron generation along the entire dorsoventral axis, the induction of ectopic MN progenitors by $Sp8$ misexpression was confined to the p3 domain. $Sp8$ misexpression in cells dorsal to the pMN domain or in floor plate cells did not result in ectopic expression of MN lineage genes (Fig. 3G; data not shown). Consistent with this observation, the generation of $En1^{+}$ V1, $Chx10$ ($Vsx2$) $^{+}$ / $Gata3^{+}$ V2 interneurons was unaffected by $Sp8$ overexpression (data not shown). These results indicate that the primary function of $Sp8$ is in establishing pMN over p3 progenitor identity. Together, these results suggest that $Sp8$ misexpression within

the p3 domain converts presumptive p3 progenitors into pMN progenitors.

Sp8 expression and the pMN domain expand ventrally in *Nkx2-2* mutants

In E10.5 *Nkx2-2* mutants, $Sp8$ expression expanded ventrally and the gap between the floor plate and the ventral boundary of $Sp8$ expression was absent (Fig. 4A–C,E–G). At this time point, *Olig2* expression also extended more ventrally, and all of the $Olig2^{+}$ cells expressed $Sp8$ (Fig. 4B,C,F,G). These $Olig2^{+}/Sp8^{+}$ cells were located next to the floor plate, indicating that the pMN domain expands ventrally without the function of *Nkx2-2*. Therefore, we conclude that the majority of the presumptive p3 progenitors are not specified but are instead converted into pMN progenitors in the absence of *Nkx2-2*. Consistent with previous studies, Pax6 expression was unaltered in *Nkx2-2* mutant embryos (Fig. 4D,H). It is known that Pax6 expression is not derepressed ventrally after loss of *Nkx2-2* or *Nkx2-2/Nkx2-9* functions (Briscoe et al., 1999; Holz et al., 2010). It is possible that the ventral limit of Pax6 expression is not controlled by *Nkx2-2*; alternatively, Pax6 expression is downregulated by *Olig2* expression, as *Olig2* expression expanded ventrally and repressed Pax6 expression in the *Nkx2-2* mutant embryos (Mizuguchi et al., 2001; Lu et al., 2002; Balaskas et al., 2012).

We also analyzed *Nkx2-2* expression patterns in both *Nestin::Cre; Sp8^{fllox/flox}* conditional knockouts and *Sp8* mutants between E10.5 and E12.5. Contrary to our expectations, the patterning of p3 and pMN progenitor domains and the generation of ventral neuronal subtypes, such as MNs, V2 and V1 interneurons, in the spinal cord appeared to be unaffected in these mice (supplementary material Fig. S4). It is possible that Pax6 expression, which is unaffected by the loss of $Sp8$ function (supplementary material Fig. S4B,F), restricts *Nkx2-2* expression.

An activator form of $Sp8$ mimics the patterning activities of the wild-type protein

Progenitor patterning in the developing spinal cord is largely mediated by transcriptional repressors (Muhr et al., 2001; Novitsch et al., 2001). To test whether the neural patterning activities of $Sp8$

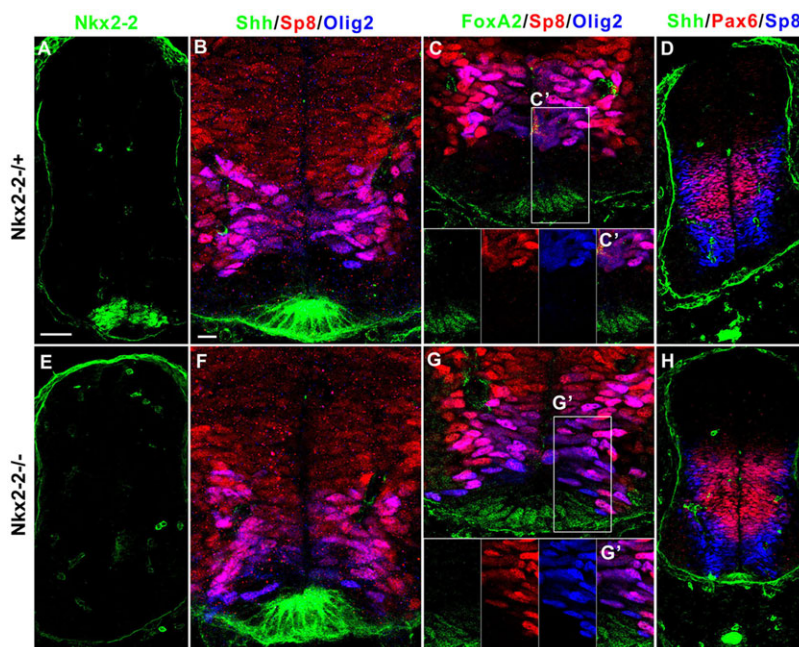


Fig. 4. $Sp8$ expression expands ventrally in *Nkx2-2* mutant mouse embryos. (A,E) No *Nkx2-2* expression was detected in the spinal cord of *Nkx2-2^{-/-}* mouse embryos compared with *Nkx2-2^{+/+}* controls. (B,C,F,G) The p3 domain, as indicated by the gap between the ventral limit of the $Olig2^{+}/Sp8^{+}$ pMN domain and the dorsal limit of the $Shh^{+}/FoxA2^{+}$ floor plate in *Nkx2-2^{+/+}* control mouse embryos, was absent in *Nkx2-2^{-/-}* embryos; $Olig2^{+}/Sp8^{+}$ cells were located adjacent to the floor plate cells. (D,H) $Sp8^{+}$, but not Pax6, expression expanded ventrally in the *Nkx2-2^{-/-}* spinal cord compared with controls. Scale bars: 50 μ m in A for A,D,E,H; 10 μ m in B for B–C',F–G'.

reflect its function as an activator or repressor, we examined whether activating (Sp8ZnF::VP16) or repressing (Sp8ZnF::EnR) forms of Sp8 could mimic the patterning activities of wild-type Sp8 (Fig. 5A).

Expression of the Sp8ZnF::VP16 fusion protein resulted in $66.2 \pm 5.3\%$ of the GFP⁺ cells within the p3 domain lacking Nkx2-2 expression (Fig. 5B,E), and $27.8 \pm 5.2\%$ of these GFP⁺ cells ectopically expressed Olig2 (Fig. 5C,E). In comparison, following Sp8 electroporation, $95.5 \pm 5.7\%$ of the GFP⁺ cells within the p3 domain lost Nkx2-2 expression as described above (Fig. 2G), with $63.3 \pm 8.6\%$ of the GFP⁺ cells exhibiting Olig2 expression (Fig. 5D,E). Thus, Sp8ZnF::VP16 possessed the patterning activities of the full-length Sp8 protein, but was less efficient. Consistent with this result, the majority of the transfected p3 progenitors retained Nkx2-2 expression following retroviral expression of Sp8ZnF::VP16, a protocol that resulted in lower levels of exogenous gene expression than electroporation in the short term (data not shown). Accordingly, Olig2 was only induced in certain retrovirally transfected bright GFP⁺ cells in the p3 domain; these Olig2⁺ cells lacked Nkx2-2 expression (data not shown). The misexpression of wild-type Sp8 using the same retrovirus resulted in Nkx2-2 repression and Olig2 induction in most of the transfected p3 progenitors (Fig. 3G). This result indicates that Sp8ZnF::VP16 only functions at higher expression levels. Notably, compared with Sp8 protein, which was primarily distributed in the nucleus of cultured cells, Sp8ZnF::VP16 protein was not confined to the nucleus but was also weakly detected in cell processes (Fig. 5F,G). The inappropriate distribution of the fusion protein most likely accounts for its weaker functions. The expression of Nkx2-2 within the p3 domain was not reduced following the misexpression of Sp8ZnF::EnR (supplementary material Fig. S5B; see below). We therefore conclude that Sp8 exerts its neural patterning activities through its function as a transcriptional activator.

A repressive form of Sp8 inhibits MN generation

Collectively, our findings suggest that Sp8 specifies the pMN over p3 progenitor fate through its function as a transcriptional activator.

We therefore considered whether a repressive form of Sp8 might interfere with endogenous Sp8 function by competitively inhibiting the expression of target genes. To examine this possibility, we tested whether the misexpression of Sp8ZnF::EnR influenced the restriction of Nkx2-2 expression dorsal to the p3 domain.

Indeed, misexpression of Sp8ZnF::EnR resulted in mild ectopic Nkx2-2 expression dorsal to the p3 domain in one-quarter of the embryos (3/13) (supplementary material Fig. S5A,B), and this was not observed in embryos electroporated with control vectors. By contrast, ectopic expression of Nkx6-1, a homeodomain transcription factor that is also expressed in the ventral spinal cord, was never found following Sp8ZnF::EnR electroporation (supplementary material Fig. S5H), indicating that the ectopic expression of Nkx2-2 is specific. These results suggest that Sp8ZnF::EnR exerts a dominant-negative effect on the Sp8 protein and interferes with the function of endogenous Sp8. Thus, restricting the dorsal limit of Nkx2-2 expression at least partially requires Sp8 function. Importantly, the expression of Nkx6-1 was even repressed following Sp8ZnF::EnR electroporation (supplementary material Fig. S5H). Consistently, Olig2 expression was also reduced by 49.7% compared with the control side, and ~80% of the GFP⁺ cells in the pMN domain no longer expressed Olig2 (supplementary material Fig. S5C,I). Moreover, ectopic Nkx2-2 expression was only induced in less than 10% of the GFP⁺ pMN domain cells (supplementary material Fig. S5C). The more pronounced Olig2 repression compared with the Nkx2-2 expansion indicates that the loss of Olig2 expression following Sp8ZnF::EnR electroporation did not result primarily from the ectopic induction of Nkx2-2 expression; Sp8 appears to be required for the induction of Olig2 expression.

Consistent with the loss of Olig2 expression within the pMN domain after the expression of Sp8ZnF::EnR, only a few GFP⁺ cells expressed the MN lineage genes *MNR2* and *Isl1*, and the number of Isl1⁺ cells was reduced by 58.3% compared with the unelectroporated control side (supplementary material Fig. S5D,E,H). By contrast, the generation of other ventral V2 and V1 interneurons was apparently

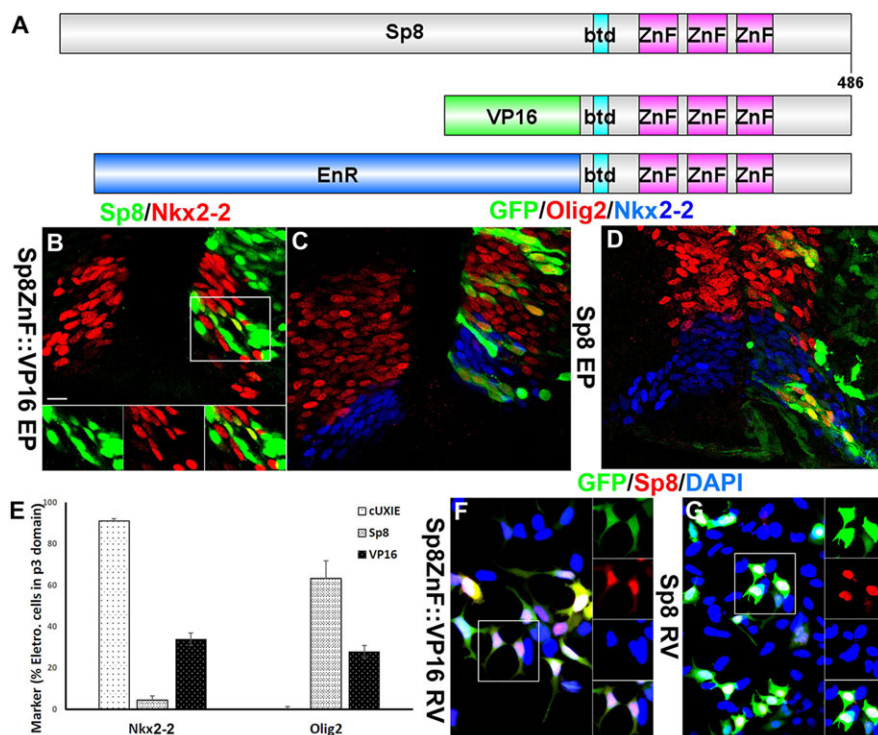


Fig. 5. Sp8 exerts its neural patterning activities by acting as a transcriptional activator. (A) Domain architecture of the wild-type Sp8, Sp8ZnF::VP16 activator and Sp8ZnF::EnR repressor proteins. ZnF, zinc-finger domain; btd, buttonhead box. (B,C) The misexpression of Sp8ZnF::VP16 following electroporation repressed Nkx2-2 in many but not all p3 domain cells (B); the induction of ectopic Olig2 expression was also detected in the p3 domain cells that lacked Nkx2-2 expression (C). (D) Following Sp8 electroporation, ectopic Olig2 expression was induced in most of the GFP⁺ cells within the p3 domain; these GFP⁺ cells lost Nkx2-2 expression. (E) Quantification of the percentage of electroporated cells in the p3 domain that expressed Nkx2-2 or Olig2 after electroporation of Sp8, cUXIE or Sp8ZnF::VP16. Error bars indicate s.e.m.; $n=3$ chickens per group. (F,G) Compared with Sp8 protein, which was primarily distributed in the nucleus (G), Sp8ZnF::VP16 protein was not confined within the nucleus as it was detected at weaker levels in the cell processes *in vitro* (F). Scale bar: 10 μ m in B for B-D,F,G.

unaffected by Sp8ZnF::EnR overexpression (supplementary material Fig. S5F–H). We conclude that Sp8 is not only required to restrict the dorsal limit of Nkx2-2 expression but also directly participates in the specification of pMN progenitor identity. Below, we discuss possible reasons why blocking Sp8 function using the mouse mutant and chick dominant-negative strategies give different results.

Sp8 expression is positively regulated by, but not completely dependent on, Pax6

Both Sp8 and Pax6 repress Nkx2-2 expression. These proteins might function through a transcriptional regulatory cascade or they might act independently. To address these possibilities, we first tested whether Sp8 regulates Pax6 expression.

We did not observe ectopic Pax6 expression ventral to its normal expression domain following Sp8 overexpression (supplementary material Fig. S6A,B), and Pax6 expression was also unaltered following Sp8ZnF::VP16 electroporation (supplementary material Fig. S6C). These results indicate that Sp8 expression does not induce Pax6 expression. Upon blocking Sp8 function with Sp8ZnF::EnR, with the exception of a few ectopic Nkx2-2⁺ cells, Pax6 expression was detected in most of the GFP⁺ transgenic cells (supplementary material Fig. S6D; data not shown), indicating that Sp8 is not required for Pax6 expression. Consistent with this result, Pax6 expression was unaffected in *Sp8* mutants (supplementary material Fig. S6E,F). Thus, Sp8 exhibits no regulatory activity on Pax6 expression, and Pax6 is unlikely to be downstream of Sp8.

We then tested whether Pax6 regulates Sp8 expression. We first checked Sp8 expression in *Sey/Sey* embryos, which contain no Pax6 protein, compared with *Sey/+* controls (Fig. 6A,D). Sp8 expression was detected at all rostrocaudal levels of the spinal cord in the

Sey/Sey embryos; however, at the rostral levels of the spinal cord a mosaic reduction in ventral Sp8 expression was observed accompanied by mosaic dorsal expansion of Nkx2-2 expression (Fig. 6B,E). Sp8 expression in the dorsal progenitors co-labeled by Pax7 remained unchanged (Fig. 6C,F). Despite the increased expression of Nkx2-2, neural progenitors nevertheless segregated into distinct populations defined by their expression of Sp8 and Nkx2-2, with fewer than 5% of the cells co-expressing both proteins (Fig. 6G,H). At caudal levels of the spinal cord, where Nkx2-2 expression did not expand dorsally, Sp8 expression was also unaltered both dorsally and ventrally (Fig. 7G). Collectively, in the *Sey/Sey* embryos, the downregulation of Sp8 expression was concurrent with the dorsal expansion of Nkx2-2 expression and with MN loss at the rostral level of the spinal cord. We then analyzed Sp8 expression patterns in chick embryos after Pax6 electroporation. Ectopic Sp8 expression was induced in 44.1±5.5% of the transgenic cells within the p3 domain (Fig. 6I). These results suggest that Sp8 expression is positively regulated by Pax6; therefore, Sp8 potentially acts downstream of Pax6 to repress Nkx2-2 expression.

In contrast to previous studies (Briscoe et al., 2000), we observed that 64% of Pax6-expressing cells within the p3 domain retained Nkx2-2 expression following Pax6 electroporation (supplementary material Fig. S7A,D). Nkx2-2 expression was only abolished in a subset of transgenic cells that expressed higher levels of Pax6, whereas Nkx2-2 remained in the cells that expressed the physiological level of Pax6, which was defined as the highest Pax6 protein level in the unelectroporated side (supplementary material Fig. S7A). The different exogenous gene expression levels that result from the different expression vectors used in this and previous studies is likely to account for the differing outcomes of the

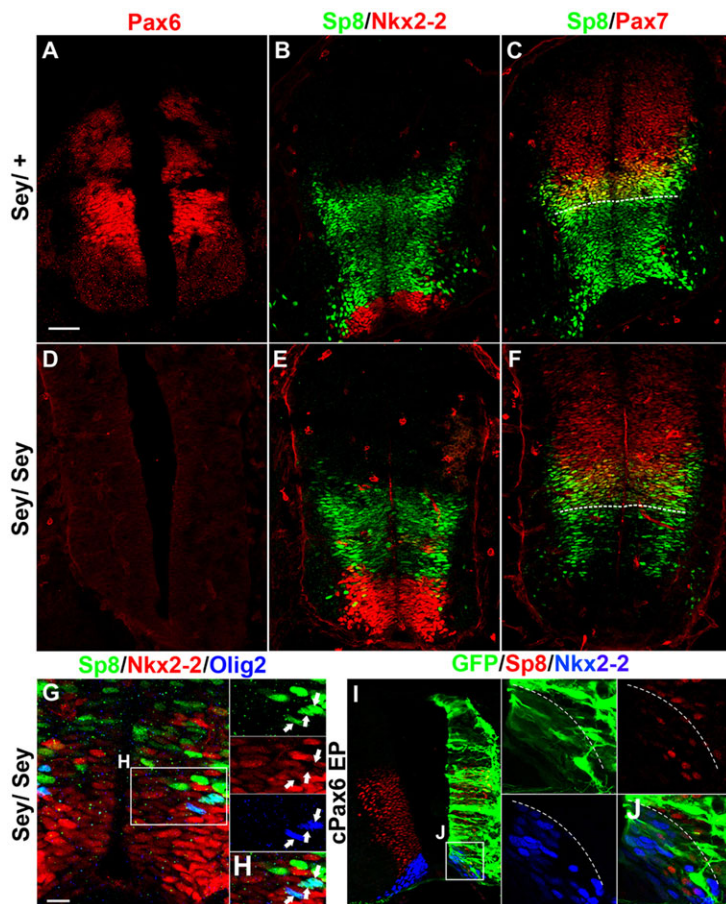


Fig. 6. Pax6 acts as a positive regulator of Sp8 expression. (A,D) No Pax6 protein was detected in the spinal cord of *Sey/Sey* mouse embryos at E10.5 (D) as compared with the *Sey/+* controls (A). (B,E) At the rostral levels of the *Sey/Sey* spinal cord, the expression of Sp8 was reduced, and this was accompanied by the mosaic dorsal expansion of Nkx2-2 expression. (C,F) Sp8 expression in Pax7-labeled dorsal progenitors appeared normal in *Sey/Sey* mutants. (G,H) The remaining Olig2⁺ cells that were interspersed among the Nkx2-2⁺ cells in *Sey/Sey* embryos expressed Sp8 but not Nkx2-2 (arrows). (I,J) After canonical Pax6 (cPax6) electroporation, Sp8 expression was induced in several transgenic cells in the p3 domain. Dashed lines indicate the p3/pMN domain boundary. Scale bars: 50 μm in A for A–F, I; 10 μm in G for G, H, J.

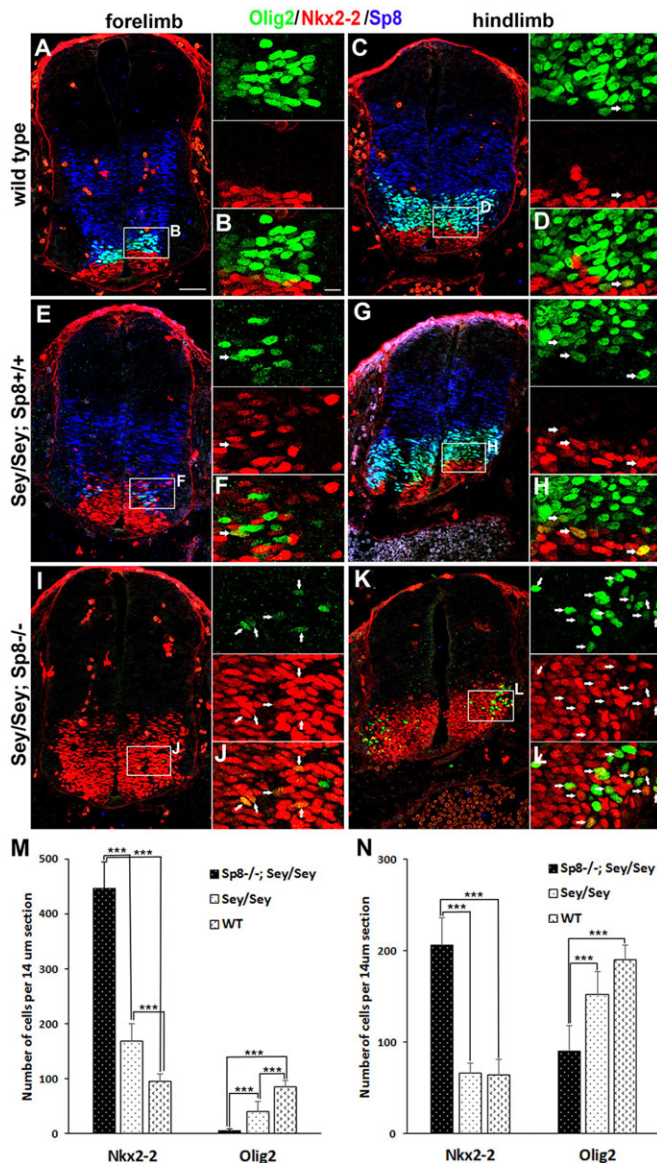


Fig. 7. Sp8 plays a supplementary role to Pax6 in establishing the pMN/p3 domain boundary. (A–D) At the forelimb and hindlimb levels of the E10.5 wild-type spinal cord, Olig2⁺ cells were located dorsal to the Nkx2-2⁺ cells; very few Olig2⁺ cells expressed Nkx2-2 at the pMN/p3 domain boundary (arrows in D). (E–H) At the forelimb levels of the E10.5 *Sey/Sey* spinal cord, Nkx2-2 expression expanded dorsally and Olig2 expression was reduced (E); at the hindlimb levels, the pMN/p3 domain was specified normally (G); very few Olig2⁺ cells expressed Nkx2-2 at either level (arrows in F,H). (I–L) At the forelimb levels of the E10.5 *Sey/Sey; Sp8^{-/-}* double-mutant spinal cord, the dorsal expansion of Nkx2-2 and the reduction of Olig2 expression were more severe than in *Sey/Sey* embryos (I); at the hindlimb levels, the pMN/p3 domain boundary was not formed (K). Along the entire rostrocaudal axis of the spinal cord, a large proportion of the Olig2⁺ cells expressed Nkx2-2 (arrows in J,L). (M,N) Quantification of the number of Nkx2-2⁺ and Olig2⁺ cells per section. Error bars indicate s.e.m.; *n*=3 embryos per group; ****P*<0.001 (one-way ANOVA). Scale bars: 50 μm in A for A–K; 10 μm in B for B–L.

Pax6 electroporation experiments. The vector that we used in the present study expressed the exogenous gene at levels that were similar to mammalian cell expression levels. In this vector, Pax6 expression is under the control of the human ubiquitin C (*UBC*) promoter. By contrast, many other vectors use promoters from viral genes, resulting in the expression of the exogenous gene at much higher than physiological levels.

We note that it is important to mimic physiological conditions when performing gain-of-function experiments for a particular gene. After Pax6 expression, 52.0% of the transgenic cells within the p3 domain ectopically expressed Olig2, and a portion of these cells did not abolish Nkx2-2 expression (36% of GFP⁺ cells co-expressed Nkx2-2 and Olig2; supplementary material Fig. S7B,D,E). Pax6 expression at high levels repressed both Sp8 and Olig2 expression (supplementary material Fig. S7C). This result is consistent with previous studies that have suggested that all neural progenitor markers are downregulated by high levels of Pax6 (Bel-Vialar et al., 2007).

Sp8 plays a supplementary role to Pax6 in establishing the pMN/p3 domain boundary

The absence of the expected expression phenotype in the *Sp8* mutant embryos raises a concern that Sp8 might not be involved in setting the boundary between the pMN and p3 domains or in MN generation. To determine whether Sp8 is physiologically relevant in this process, we compared the expression patterns of Nkx2-2 and Olig2 in *Sp8^{-/-}*; *Sey/Sey* double mutants and *Sey/Sey* single mutants.

At E10.5, we observed a more robust dorsal expansion of Nkx2-2 expression and MN loss along the entire rostrocaudal axis of the spinal cord in the *Sp8^{-/-}*; *Sey/Sey* embryos compared with the *Sey/Sey* embryos. At the forelimb levels of the spinal cord, Nkx2-2 expression was confined to the p3 domain in the wild-type control mice (Fig. 7A); however, its expression extended dorsally and occupied nearly one-third of the dorsoventral axis of the spinal cord in both the *Sey/Sey* and *Sp8^{-/-}*; *Sey/Sey* embryos (Fig. 7E,I,M), and the density of ectopic Nkx2-2⁺ cells was greatly increased in the *Sp8^{-/-}*; *Sey/Sey* embryos (Fig. 7I,M) compared with the *Sey/Sey* embryos (Fig. 7E,M). At the hindlimb levels of the spinal cord, the dorsal expansion of Nkx2-2 expression was also observed in *Sp8^{-/-}*; *Sey/Sey* embryos (Fig. 7K,N) but not in wild-type or *Sey/Sey* embryos (Fig. 7C,G,N).

Concurrent with the robust dorsal expansion of Nkx2-2 expression, a much greater reduction in Olig2 expression was observed in *Sp8^{-/-}*; *Sey/Sey* than in *Sey/Sey* embryos (Fig. 7E–N). Moreover, the vast majority of the remaining Olig2⁺ pMN progenitors that were interspersed among Nkx2-2⁺ cells in the *Sey/Sey* embryos has lost Nkx2-2 expression (Fig. 7E); however, 44.0% of these Olig2⁺ cells expressed Nkx2-2 after the loss of both Sp8 and Pax6 functions in the *Sp8^{-/-}*; *Sey/Sey* embryos (Fig. 7I,K), indicating that the remaining Sp8 expression extinguished Nkx2-2 expression from the pMN progenitors in *Sey/Sey* embryos. Overall, these results suggest that the loss of function of Pax6 alone results in the disruption of the pMN/p3 domain boundary only at the rostral levels of the spinal cord; however, loss of function of both Pax6 and Sp8 results in the disruption of the pMN/p3 domain boundary along the entire rostrocaudal axis of the spinal cord. Thus, we conclude that both Sp8 and Pax6 are involved in the repression of Nkx2-2 expression.

The clearance of Nkx2-2 expression from pMN progenitors is crucial for the specification of MN fate

Sp8 and Nkx2-2 exert opposing effects on MN fate specification. The gene interaction pathway was determined by performing epistasis experiments, in which we co-electroporated Sp8 in combination with Nkx2-2 into chick embryos. This electroporation resulted in the co-expression of Sp8 and Nkx2-2 in ~90% of the GFP⁺ cells (supplementary material Fig. S8C).

Consistent with previous studies, Nkx2-2 misexpression completely abolished Olig2 expression (supplementary material Fig. S8A,B). The re-expression of Nkx2-2 in p3 progenitors completely blocked the ability of Sp8 to induce ectopic MNs in the

p3 domain, as none of the *Nkx2-2*^{+/GFP} cells within the p3 domain expressed *Olig2* or *Isl1* (supplementary material Fig. S8B; data not shown). By contrast, *Sp8* expression did not rescue the MN generation defects that resulted from *Nkx2-2* misexpression in the pMN progenitors. This conclusion was reached given that (1) GFP⁺ cells in the pMN domain never expressed *Olig2*, and (2) GFP⁺ cells in the mantle zone never expressed *Isl1*, regardless of *Sp8* expression (supplementary material Fig. S8D; data not shown). These results suggest that the clearance of *Nkx2-2* expression from pMN progenitors is crucial for them to attain the MN fate, indicating the importance of *Sp8* function in controlling the dorsal limit of *Nkx2-2* expression.

DISCUSSION

Cross-repressive interactions are fundamental to the mechanisms that underlie the specification of cell identities during embryonic development. In the present study, we demonstrate that *Sp8* plays a supplementary role to *Pax6* in specifying the dorsal limit of the p3 progenitor domain boundary by repressing *Nkx2-2* expression in the adjacent pMN progenitor domain. Our conclusions are supported by the following results: (1) the ventral limit of *Sp8* expression is complementary to the dorsal limit of *Nkx2-2* expression at the pMN/p3 boundary; (2) gain-of-function experiments in chick embryos reveal that *Sp8* and *Nkx2-2* exert cross-repressive interactions and that changing the expression of *Sp8* and *Nkx2-2* is coupled with pMN and p3 progenitor fate conversion; (3) the loss of *Nkx2-2* function leads to ectopic expression of *Sp8* in the p3 domain; (4) blocking *Sp8* function via a dominant-negative strategy leads to a dorsal expansion of *Nkx2-2* expression; and (5) the loss of function of *Pax6* alone results in the disruption of the pMN/p3 domain boundary only at rostral levels of the spinal cord, whereas loss of function of both *Pax6* and *Sp8* results in disruption of the pMN/p3 domain boundary along the entire rostrocaudal axis of the spinal cord.

Specification of pMN/p3 progenitor identities

Recent studies have shown that ~90% of pMN cells are lineage traced in *Nkx2-2*^{p3-CRM::Cre} mice, indicating that this *Nkx2-2* enhancer is initially activated in the pMN progenitors (Wang et al., 2011). Similarly, *Olig2* and *Olig1* lineage-tracing experiments using *Cre* knock-in mice suggest that *Olig2* and *Olig1* are transiently activated in the *Nkx2-2*⁺ p3 progenitors (Wu et al., 2006; Dessaud et al., 2007; Chen et al., 2011). Thus, the pMN and the p3 progenitors share a common origin: the *Olig2*⁺/*Nkx2-2*⁺ cells. These cells undergo a refining patterning step, during which *Nkx2-2* expression is selectively repressed in the pMN domain and *Olig2* expression is selectively repressed in the p3 domain. *Nkx2-2* represses *Olig2* expression and is responsible for the clearance of *Olig2* from the p3 domain, but *Olig2* expression does not repress *Nkx2-2* expression. Thus, a gene other than *Olig2* might clear *Nkx2-2* expression from the pMN domain. The dorsal expansion of *Nkx2-2* expression at the rostral levels of the spinal cord after the loss of *Pax6* function suggests that *Pax6* contributes to repressing *Nkx2-2* expression in the pMN domain.

In the present study, we found that *Sp8* is also involved in repressing *Nkx2-2* expression. The overexpression of *Sp8* repressed *Nkx2-2*. The more robust dorsal expansion of *Nkx2-2* expression in *Sp8*^{-/-}; *Sey/Sey* embryos compared with *Sey/Sey* embryos suggests that *Sp8* plays a supplementary role in repressing *Nkx2-2* expression. Thus, both *Sp8* and *Pax6* participate in the clearance of *Nkx2-2* expression from the pMN domains, which is essential for the maintenance of *Olig2* expression and creates competency for the production of MNs.

Pax6 expression was unaltered following gain or loss of *Sp8* function, indicating that *Pax6* is not regulated by *Sp8*; however, the reduction of *Sp8* expression in the *Sey/Sey* mutants and the induction of *Sp8* in the p3 domains following *Pax6* overexpression suggest that *Sp8* expression is positively regulated by *Pax6*. Although *Pax6* plays a positive role in *Sp8* expression, it is not required, suggesting that there might be other inputs regulating *Sp8*.

The initiation of *Olig2* expression is activated by Shh-Gli signaling through the Gli binding site in the *Olig2* promoter (Peterson et al., 2012). *Olig2* expression is initiated in the floor plate, p3, pMN and p2 domains; however, the *Nkx2-2* expression that is later activated by Shh-Gli signaling extinguishes *Olig2* expression from the floor plate and the p3 domain (Dessaud et al., 2007). A balance between the activation and repression of *Olig2* expression appears likely. *Pax6* overexpression induces *Olig2* expression in the p3 domain cells without clearance of its repressor *Nkx2-2*, indicating that activation by *Pax6* overrides repression by *Nkx2-2* of *Olig2* expression. *Sp8* strongly represses *Nkx2-2* expression and maintains *Olig2* expression by clearance of *Nkx2-2*. *Sp8* also appears to activate *Olig2* expression independently of its repression of *Nkx2-2*, as numerous pMN domain cells lost *Olig2* expression without ectopic *Nkx2-2* induction after blocking *Sp8* function with *Sp8ZnF::EnR*.

Both *Sp8* and *Pax6* are expressed much more broadly than *Olig2* but only induce *Olig2* expression in the ventralmost neuronal progenitor domains. *Sp8* and *Pax6* might only act synergistically with graded Shh-Gli signaling and, in more dorsal regions, the lower Shh concentration might be insufficient to initiate *Olig2* expression. Moreover, *Olig2* expression is extinguished by *Irx3* in the p2 domain through induction of *Mir-17-3p*, which directly targets and silences *Olig2* mRNA (Chen et al., 2011).

Sp8 functions as an activator to pattern the ventral spinal cord

The majority of the progenitor transcription factors that have been implicated in ventral neural tube patterning function as direct repressors and exert this effect by recruiting the Gro/TEL co-repressor through their engrailed homology-1 (eh1) domains (Muhr et al., 2001). In the present study, we demonstrated that the chimeric protein *Sp8ZnF::VP16* mimics the patterning activities of full-length *Sp8*; however, *Sp8ZnF::EnR* did not repress *Nkx2-2* expression. This indicates that *Sp8* functions through its activator activity. *Sp8* is not the only progenitor transcription factor that functions as an activator. For example, *Irx3* lacks eh1 motifs and establishes the p2/pMN boundary through cross-repressive interactions with *Olig2*, and recent studies demonstrate that *Irx3* induces *Mir-17-3p* expression, which silences *Olig2* mRNA (Chen et al., 2011). *Pax6* has also been shown to pattern the ventral spinal cord through its activator activities (Muhr et al., 2001).

Sp9 may compensate for Sp8 in Sp8 mutant embryos

In the present study, although the pMN/p3 domain boundary was disrupted along the entire rostrocaudal axis of the spinal cord in *Sp8*^{-/-}; *Sey/Sey* embryos, a substantial number of *Olig2*⁺ cells were still present. More than half of these *Olig2*⁺ cells did not turn on *Nkx2-2* expression, suggesting that they might have a pMN progenitor identity. There are several possibilities as to how this phenotype might arise. First, a delay in the onset of *Nkx2-2* expression could lead to persistent *Olig2* expression. Alternatively, a gene other than *Pax6* or *Sp8* might account for the repression of *Nkx2-2* expression.

The loss of Sp8 function (in *Sp8*^{−/−} mutants) did not impair the specification of pMN/p3 progenitors, whereas blocking Sp8 function using a dominant-negative strategy resulted in defects in pMN progenitor specification and in a mild dorsal expansion of *Nkx2-2* expression. These differing results might have been due to off-target effects of the Sp8ZnF::EnR construct, perhaps interfering with the functions of both Sp8 and Sp9. Only one amino acid residue differs between Sp8 and Sp9 within the zinc-finger domain. Thus, these two proteins might bind to the same genes and serve several redundant roles. Indeed, following Sp9 overexpression, we observed that Sp9 displayed overlapping functions with Sp8 in restricting *Nkx2-2* expression and in specifying pMN progenitor fate (data not shown). Therefore, Sp9 might compensate for the loss of Sp8 in *Sp8* mutant embryos, whereas both Sp8 and Sp9 functions might be blocked by Sp8ZnF::EnR in our experiments. Future studies are needed to examine neural tube patterning in *Sp8* and *Sp9* double mutants.

MATERIALS AND METHODS

DNA constructs

All coding sequences were cloned into the retroviral expression vector cUXIE (provided by H. Song, The Johns Hopkins University, USA) in order to co-express a transgene and *GFP* under the human *UBC* promoter. The primers used for gene cloning are listed in supplementary material Table S2. The coding sequence of the VP16 activation domain (VP16) was ligated to the Sp8 zinc-finger domain by overlapping PCR. Canonical *Pax6* was amplified by overlapping PCR from *Pax6(5a)* (purchased from OriGene). All constructs were confirmed by sequencing.

In ovo electroporation and retrovirus injection

All experiments using animals were performed in accordance with institutional guidelines. Fertilized chicken eggs were incubated in a humidified, forced-draft incubator at 37.8°C. Plasmid DNA was electroporated into Hamburger and Hamilton (HH) stage 11–12 chick embryos. At 36–48 h post transfection embryos were collected. In co-electroporation experiments, the constructs were mixed at a ratio of 1:1. Replication-incompetent retrovirus was packaged and co-transfected with cUXIE and VSV-G (Clontech, PT3343-5) plasmids into the GP2-293 cell line using the calcium phosphate method.

Immunohistochemistry and imaging

For staging mouse embryos, noon on the day of plug confirmation was defined as embryonic day (E) 0.5. Embryos were collected in 0.1 M PBS on ice and fixed for 30 min to 2 h with 4% paraformaldehyde in 0.1 M phosphate buffer (PB) and then washed twice for 10 min each, immersed in 30% sucrose/0.1 M PB and frozen in embedding medium (O.C.T., Sakura Finetek). Serial sections of 14–20 µm were then cut and collected on Fisher Colorfrost-Plus slides. Immunohistochemistry was performed as previously described (Li et al., 2011b). Primary antibodies (supplementary material Table S1) were incubated overnight. The following secondary antibodies were used: donkey anti-goat Alexa Fluor 488 (Molecular Probes, A-11055, 1:600), donkey anti-goat Alexa Fluor 555 (Molecular Probes, A-21432, 1:600), donkey anti-goat Alexa Fluor 633 (Molecular Probes, A-21082, 1:600), donkey anti-mouse Cy2 (Jackson, 715-225-151, 1:300), donkey anti-mouse Cy3 (Jackson, 715-165-151, 1:300), donkey anti-mouse Cy3 (Jackson, 715-175-151, 1:300), donkey anti-rabbit Cy2 (Jackson, 711-225-152, 1:300), donkey anti-rabbit Cy3 (Jackson, 711-165-152, 1:300) and donkey anti-rabbit Cy5 (Jackson, 711-175-152, 1:300). Secondary antibodies were incubated for 2 h. All sections were counterstained with DAPI (Sigma, 400 ng/ml, 5 min). Images were collected using an Olympus FV1000 confocal microscope.

Transgenic mouse strains

Nestin::Cre mice and EIIA::Cre mice were genotyped by PCR using generic *Cre* primers. *Shh*::Cre mice (which carry an *Shh* null allele) were genotyped

as previously described (Harfe et al., 2004). *Sp8* floxed mice were provided by K. Campbell (University of Cincinnati) and genotyped as described (Waclaw et al., 2006). *Sp8* mutant mice were generated by crossing *Sp8* floxed mice with EIIA::Cre mice as previously described (Bell et al., 2003). *Nkx2-2* mutant mice (Sussel et al., 1998) were genotyped by PCR using the following primers: *Nkx2-2* sense, CAGAGCCATGACCAAGAA; *Nkx2-2* antisense, GCCTAGTTGACCTCTTCG; PGK antisense, GAAAGCGAA-GGAGCAAAG. *Sev/Sev* mice were genotyped by eye defects.

Data quantification

A total of three samples were used for each group and three sections were counted for each sample. Results are presented as mean±s.e.m. Statistical significance was evaluated by Student's *t*-test or one-way ANOVA. *P*<0.05 was considered significant.

Acknowledgements

We thank Dr John Rubenstein for comments and suggestions; Dr Kenneth Campbell for the *Sp8* floxed mice and the *Sp9* *in situ* hybridization probe; Dr Hongjun Song for providing the cUXIE retroviral expression vector; and Dr Juan Carlos Izpisua Belmonte for mouse and chick *Sp8* probes.

Competing interests

The authors declare no competing financial interests.

Author contributions

X.L., M.Q. and Z.Y. conceived the project and designed experiments; X.L. and Z.L. performed experiments; X.L. and Z.Y. analyzed and discussed the data; X.L. and Z.Y. wrote the manuscript.

Funding

This work was supported by the National Basic Research Program of China [grants 2011CB504400 and 2013CB531300] and the National Natural Science Foundation of China [grants 31121061 and 91232723].

Supplementary material

Supplementary material available online at <http://dev.biologists.org/lookup/suppl/doi:10.1242/dev.105387/-/DC1>

References

- Alaynick, W. A., Jessell, T. M. and Pfaff, S. L. (2011). SnapShot: spinal cord development. *Cell* **146**, 178–178 e1.
- Balaskas, N., Ribeiro, A., Panovska, J., Dessaud, E., Sasai, N., Page, K. M., Briscoe, J. and Ribes, V. (2012). Gene regulatory logic for reading the Sonic Hedgehog signaling gradient in the vertebrate neural tube. *Cell* **148**, 273–284.
- Bel-Vialar, S., Medevielle, F. and Pituello, F. (2007). The on/off of Pax6 controls the tempo of neuronal differentiation in the developing spinal cord. *Dev. Biol.* **305**, 659–673.
- Bell, S. M., Schreiner, C. M., Waclaw, R. R., Campbell, K., Potter, S. S. and Scott, W. J. (2003). Sp8 is crucial for limb outgrowth and neuropore closure. *Proc. Natl. Acad. Sci. U.S.A.* **100**, 12195–12200.
- Briscoe, J. and Ericson, J. (1999). The specification of neuronal identity by graded Sonic Hedgehog signalling. *Semin. Cell Dev. Biol.* **10**, 353–362.
- Briscoe, J., Sussel, L., Serup, P., Hartigan-O'Connor, D., Jessell, T. M., Rubenstein, J. L. R. and Ericson, J. (1999). Homeobox gene *Nkx2.2* and specification of neuronal identity by graded Sonic hedgehog signalling. *Nature* **398**, 622–627.
- Briscoe, J., Pierani, A., Jessell, T. M. and Ericson, J. (2000). A homeodomain protein code specifies progenitor cell identity and neuronal fate in the ventral neural tube. *Cell* **101**, 435–445.
- Chamberlain, C. E., Jeong, J., Guo, C., Allen, B. L. and McMahon, A. P. (2008). Notochord-derived Shh concentrates in close association with the apically positioned basal body in neural target cells and forms a dynamic gradient during neural patterning. *Development* **135**, 1097–1106.
- Chen, J.-A., Huang, Y.-P., Mazzoni, E. O., Tan, G. C., Zavadil, J. and Wichterle, H. (2011). Mir-17-3p controls spinal neural progenitor patterning by regulating Olig2/Irx3 cross-repressive loop. *Neuron* **69**, 721–735.
- Dasen, J. S., De Camilli, A., Wang, B., Tucker, P. W. and Jessell, T. M. (2008). Hox repertoires for motor neuron diversity and connectivity gated by a single accessory factor, FoxP1. *Cell* **134**, 304–316.
- Dessaud, E., Yang, L. L., Hill, K., Cox, B., Ulloa, F., Ribeiro, A., Mynett, A., Novitsch, B. G. and Briscoe, J. (2007). Interpretation of the sonic hedgehog morphogen gradient by a temporal adaptation mechanism. *Nature* **450**, 717–720.
- Dessaud, E., McMahon, A. P. and Briscoe, J. (2008). Pattern formation in the vertebrate neural tube: a sonic hedgehog morphogen-regulated transcriptional network. *Development* **135**, 2489–2503.

- Dessaud, E., Ribes, V., Balaskas, N., Yang, L. L., Pierani, A., Kicheva, A., Novitsch, B. G., Briscoe, J. and Sasai, N. (2010). Dynamic assignment and maintenance of positional identity in the ventral neural tube by the morphogen sonic hedgehog. *PLoS Biol.* **8**, e1000382.
- Ericson, J., Briscoe, J., Rashbass, P., van Heyningen, V. and Jessell, T. M. (1997a). Graded sonic hedgehog signaling and the specification of cell fate in the ventral neural tube. *Cold Spring Harb. Symp. Quant. Biol.* **62**, 451-466.
- Ericson, J., Rashbass, P., Schedl, A., Brenner-Morton, S., Kawakami, A., van Heyningen, V., Jessell, T. M. and Briscoe, J. (1997b). Pax6 controls progenitor cell identity and neuronal fate in response to graded Shh signaling. *Cell* **90**, 169-180.
- Flames, N., Pla, R., Gelman, D. M., Rubenstein, J. L. R., Puelles, L. and Marin, O. (2007). Delineation of multiple subpallial progenitor domains by the combinatorial expression of transcriptional codes. *J. Neurosci.* **27**, 9682-9695.
- Harfe, B. D., Scherz, P. J., Nissim, S., Tian, H., McMahon, A. P. and Tabin, C. J. (2004). Evidence for an expansion-based temporal Shh gradient in specifying vertebrate digit identities. *Cell* **118**, 517-528.
- Holz, A., Kollmus, H., Ryge, J., Niederkofler, V., Dias, J., Ericson, J., Stoeckli, E. T., Kiehn, O. and Arnold, H.-H. (2010). The transcription factors Nkx2.2 and Nkx2.9 play a novel role in floor plate development and commissural axon guidance. *Development* **137**, 4249-4260.
- Jacob, J. and Briscoe, J. (2003). Gli proteins and the control of spinal-cord patterning. *EMBO Rep.* **4**, 761-765.
- Jeong, J. and McMahon, A. P. (2005). Growth and pattern of the mammalian neural tube are governed by partially overlapping feedback activities of the hedgehog antagonists patched 1 and Hhip1. *Development* **132**, 143-154.
- Kawakami, Y., Esteban, C. R., Matsui, T., Rodríguez-León, J., Kato, S. and Izpisua Belmonte, J. C. (2004). Sp8 and Sp9, two closely related buttonhead-like transcription factors, regulate Fgf8 expression and limb outgrowth in vertebrate embryos. *Development* **131**, 4763-4774.
- Lee, S.-K. and Pfaff, S. L. (2001). Transcriptional networks regulating neuronal identity in the developing spinal cord. *Nat. Neurosci.* **4** Suppl, 1183-1191.
- Lek, M., Dias, J. M., Marklund, U., Uhde, C. W., Kurdija, S., Lei, Q., Sussel, L., Rubenstein, J. L., Matisse, M. P., Arnold, H.-H. et al. (2010). A homeodomain feedback circuit underlies step-function interpretation of a Shh morphogen gradient during ventral neural patterning. *Development* **137**, 4051-4060.
- Li, H., de Faria, J. P., Andrew, P., Nitarska, J. and Richardson, W. D. (2011a). Phosphorylation regulates OLIG2 cofactor choice and the motor neuron-oligodendrocyte fate switch. *Neuron* **69**, 918-929.
- Li, X., Sun, C., Lin, C., Ma, T., Madhavan, M. C., Campbell, K. and Yang, Z. (2011b). The transcription factor Sp8 is required for the production of parvalbumin-expressing interneurons in the olfactory bulb. *J. Neurosci.* **31**, 8450-8455.
- Liem, K. F., Jr, Jessell, T. M. and Briscoe, J. (2000). Regulation of the neural patterning activity of sonic hedgehog by secreted BMP inhibitors expressed by notochord and somites. *Development* **127**, 4855-4866.
- Litingtung, Y. and Chiang, C. (2000). Specification of ventral neuron types is mediated by an antagonistic interaction between Shh and Gli3. *Nat. Neurosci.* **3**, 979-985.
- Lu, Q. R., Yuk, D.-i., Alberta, J. A., Zhu, Z., Pawlitzky, I., Chan, J., McMahon, A. P., Stiles, C. D. and Rowitch, D. H. (2000). Sonic hedgehog-regulated oligodendrocyte lineage genes encoding bHLH proteins in the mammalian central nervous system. *Neuron* **25**, 317-329.
- Lu, Q. R., Sun, T., Zhu, Z., Ma, N., Garcia, M., Stiles, C. D. and Rowitch, D. H. (2002). Common developmental requirement for Olig function indicates a motor neuron/oligodendrocyte connection. *Cell* **109**, 75-86.
- Marquardt, T. and Gruss, P. (2002). Generating neuronal diversity in the retina: one for nearly all. *Trends Neurosci.* **25**, 32-38.
- Marti, E., Takada, R., Bumcrot, D. A., Sasaki, H. and McMahon, A. P. (1995). Distribution of Sonic hedgehog peptides in the developing chick and mouse embryo. *Development* **121**, 2537-2547.
- Mizuguchi, R., Sugimori, M., Takebayashi, H., Kosako, H., Nagao, M., Yoshida, S., Nabeshima, Y.-i., Shimamura, K. and Nakafuku, M. (2001). Combinatorial roles of olig2 and neurogenin2 in the coordinated induction of pan-neuronal and subtype-specific properties of motoneurons. *Neuron* **31**, 757-771.
- Muhr, J., Andersson, E., Persson, M., Jessell, T. M. and Ericson, J. (2001). Groucho-mediated transcriptional repression establishes progenitor cell pattern and neuronal fate in the ventral neural tube. *Cell* **104**, 861-873.
- Novitsch, B. G., Chen, A. I. and Jessell, T. M. (2001). Coordinate regulation of motor neuron subtype identity and pan-neuronal properties by the bHLH repressor Olig2. *Neuron* **31**, 773-789.
- Pearson, B. J. and Doe, C. Q. (2004). Specification of temporal identity in the developing nervous system. *Annu. Rev. Cell Dev. Biol.* **20**, 619-647.
- Persson, M., Stamatakis, D., te Welscher, P., Andersson, E., Bose, J., Ruther, U., Ericson, J. and Briscoe, J. (2002). Dorsal-ventral patterning of the spinal cord requires Gli3 transcriptional repressor activity. *Genes Dev.* **16**, 2865-2878.
- Peterson, K. A., Nishi, Y., Ma, W., Vedenko, A., Shokri, L., Zhang, X., McFarlane, M., Baizabal, J.-M., Junker, J. P., van Oudenaarden, A. et al. (2012). Neural-specific Sox2 input and differential Gli-binding affinity provide context and positional information in Shh-directed neural patterning. *Genes Dev.* **26**, 2802-2816.
- Pierani, A., Brenner-Morton, S., Chiang, C. and Jessell, T. M. (1999). A sonic hedgehog-independent, retinoid-activated pathway of neurogenesis in the ventral spinal cord. *Cell* **97**, 903-915.
- Roussou, D. L., Gaber, Z. B., Wellik, D., Morrissey, E. E. and Novitsch, B. G. (2008). Coordinated actions of the forkhead protein Foxp1 and Hox proteins in the columnar organization of spinal motor neurons. *Neuron* **59**, 226-240.
- Shen, Q., Wang, Y., Dimos, J. T., Fasano, C. A., Phoenix, T. N., Lemischka, I. R., Ivanova, N. B., Stifani, S., Morrissey, E. E. and Temple, S. (2006). The timing of cortical neurogenesis is encoded within lineages of individual progenitor cells. *Nat. Neurosci.* **9**, 743-751.
- Stamatakis, D., Ulloa, F., Tsoni, S. V., Mynett, A. and Briscoe, J. (2005). A gradient of Gli activity mediates graded Sonic Hedgehog signaling in the neural tube. *Genes Dev.* **19**, 626-641.
- Sussel, L., Kalamaras, J., Hartigan-O'Connor, D. J., Meneses, J. J., Pedersen, R. A., Rubenstein, J. L. and German, M. S. (1998). Mice lacking the homeodomain transcription factor Nkx2.2 have diabetes due to arrested differentiation of pancreatic beta cells. *Development* **125**, 2213-2221.
- Treichel, D., Schöck, F., Jäckle, H., Gruss, P. and Mansouri, A. (2003). mBtd is required to maintain signaling during murine limb development. *Genes Dev.* **17**, 2630-2635.
- Waclaw, R. R., Allen, Z. J., II, Bell, S. M., Erdélyi, F., Szabó, G., Potter, S. S. and Campbell, K. (2006). The zinc finger transcription factor Sp8 regulates the generation and diversity of olfactory bulb interneurons. *Neuron* **49**, 503-516.
- Wang, H., Lei, Q., Oosterveen, T., Ericson, J. and Matisse, M. P. (2011). Tcf/Lef repressors differentially regulate Shh-Gli target gene activation thresholds to generate progenitor patterning in the developing CNS. *Development* **138**, 3711-3721.
- Wu, S., Wu, Y. and Capecchi, M. R. (2006). Motoneurons and oligodendrocytes are sequentially generated from neural stem cells but do not appear to share common lineage-restricted progenitors in vivo. *Development* **133**, 581-590.
- Zhou, Q. and Anderson, D. J. (2002). The bHLH transcription factors OLIG2 and OLIG1 couple neuronal and glial subtype specification. *Cell* **109**, 61-73.
- Zhou, Q., Wang, S. and Anderson, D. J. (2000). Identification of a novel family of oligodendrocyte lineage-specific basic helix-loop-helix transcription factors. *Neuron* **25**, 331-343.
- Zhou, Q., Choi, G. and Anderson, D. J. (2001). The bHLH transcription factor Olig2 promotes oligodendrocyte differentiation in collaboration with Nkx2.2. *Neuron* **31**, 791-807.

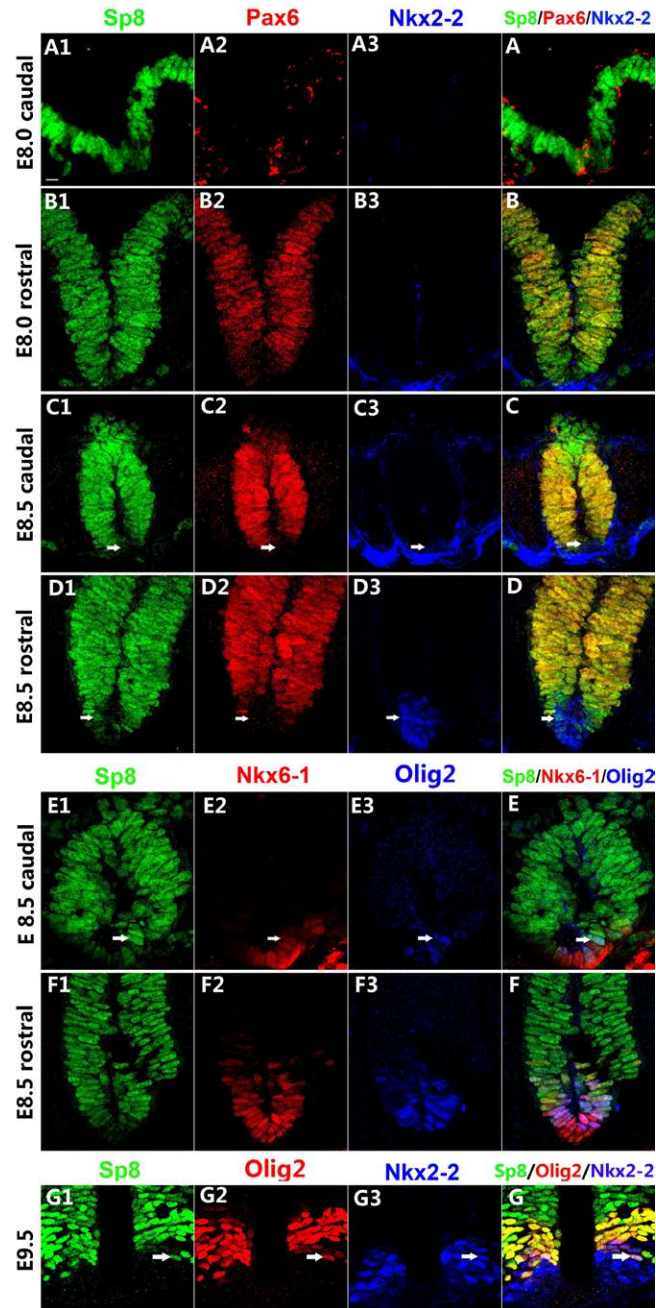


Figure S1. The temporal specification of the p3/pMN domain boundary. (A1-B) The expression patterns of Sp8, Pax6 and Nkx2-2 in the mouse caudal (A1-A) and rostral (B1-B) neural plate at E8.0. Note that only Sp8 was detected at caudal levels. (C1-D) At E8.5, Nkx2-2 was first detected in the ventral midline. Sp8 but not Pax6 was expressed in some Nkx2-2+ cells (arrows). (E1-F) The expression patterns of Sp8, Nkx6-1 and Olig2 in rostral and caudal spinal cord at E8.5. (G1-G) At E9.5, Sp8, Olig2 and Nkx2-2 triple-labeled cell can be still observed at the p3/pMN domain boundary (arrows). Scale bar: 10 μ m (shown in A1, applies to A1-G).

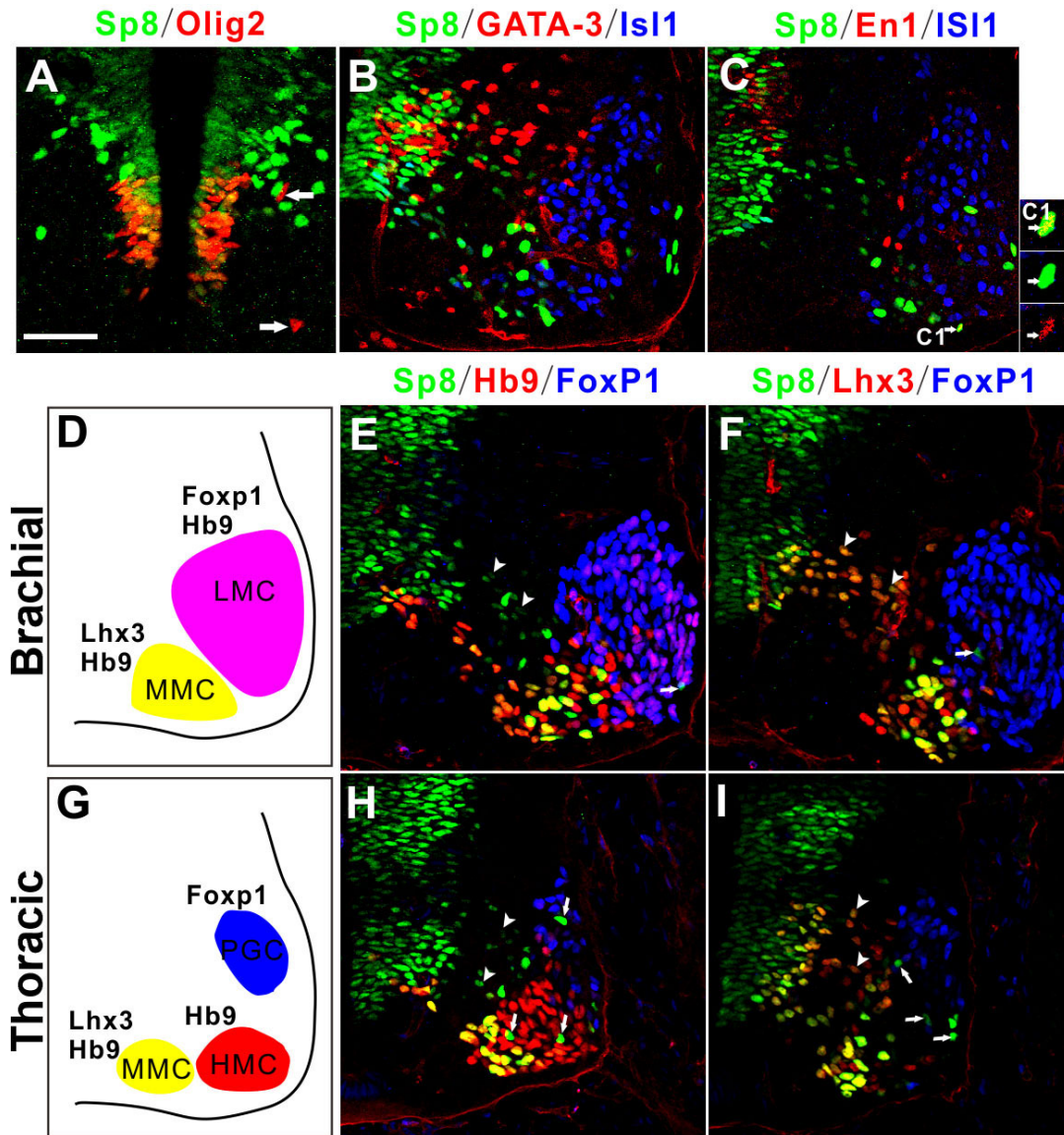


Figure S2. Sp8 is expressed by several types of ventral neurons in the mouse spinal cord at E12.0-12.5. (A) At E12.5, Olig2+ cells in the VZ co-expressed Sp8, but Olig2+ oligodendrocytes (arrows) that migrated outside of the VZ no longer expressed Sp8 protein. (B) Sp8 expression was not detected in the GATA-3+ V2 interneurons. (C, C1) Sp8 expression was detected in a subpopulation of En1+ V1 interneurons (arrows). (D, G) Schematic diagrams illustrating motor columns at the brachial levels (D) and thoracic levels (G) of the spinal cord defined by the combinatorial expression of three transcription factors Lhx3, FoxP1 and Hb9. (E, F, H, I) At the brachial and thoracic levels, only MMC MNs expressed Sp8, but Sp8+ cells within the LMC at the brachial level and within the HMC and PGC at the thoracic level did not express any of these MN markers (arrows). Sp8 was also expressed in Lhx3+/Hb9- V2 interneurons (arrowheads). Scale bars: 50 μm (shown in A, applies to A, C'); 10 μm (shown in B, applies to B, C, E, F, H, I).

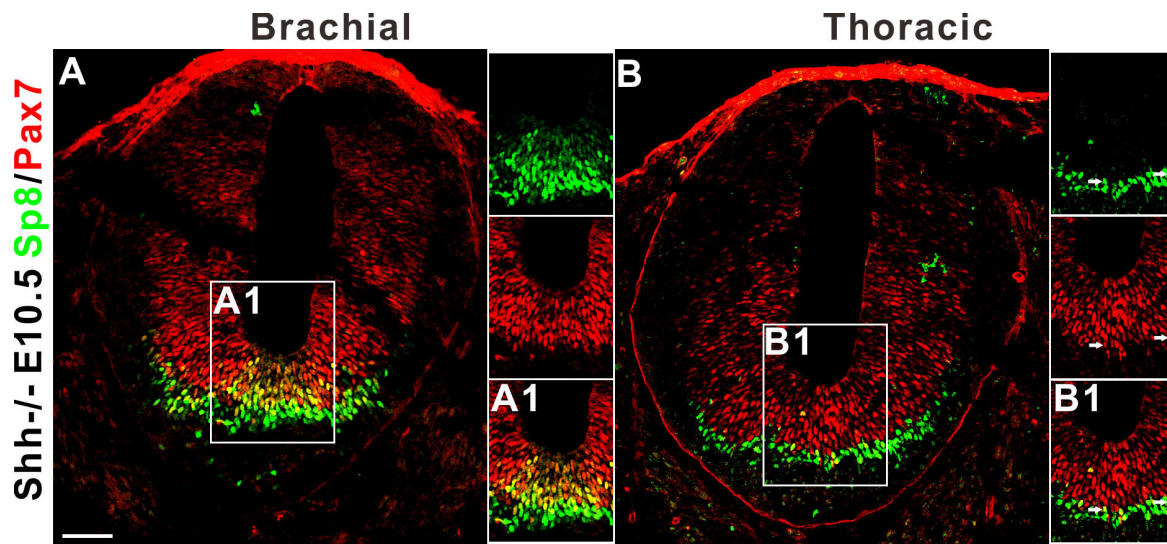


Figure S3. Sp8 expression expands into the ventral midline of the spinal cord of E10.5 *Shh*^{-/-} mouse embryos. (A) At the brachial levels of the ventral midline of the spinal cord in E10.5 *Shh*^{-/-} mice, Sp8 was expressed in the VZ and SVZ. In the VZ, nearly all of the Sp8⁺ cells expressed Pax7 and vice versa. **(B)** At the thoracic levels, Sp8 was primarily expressed in the SVZ. Sp8⁺ cells formed a crescent; only a small number of Sp8⁺ cells expressed Pax7 (arrows in B1). Scale bar: 50 μ m (shown in A, applies to A, A1, B, B1).

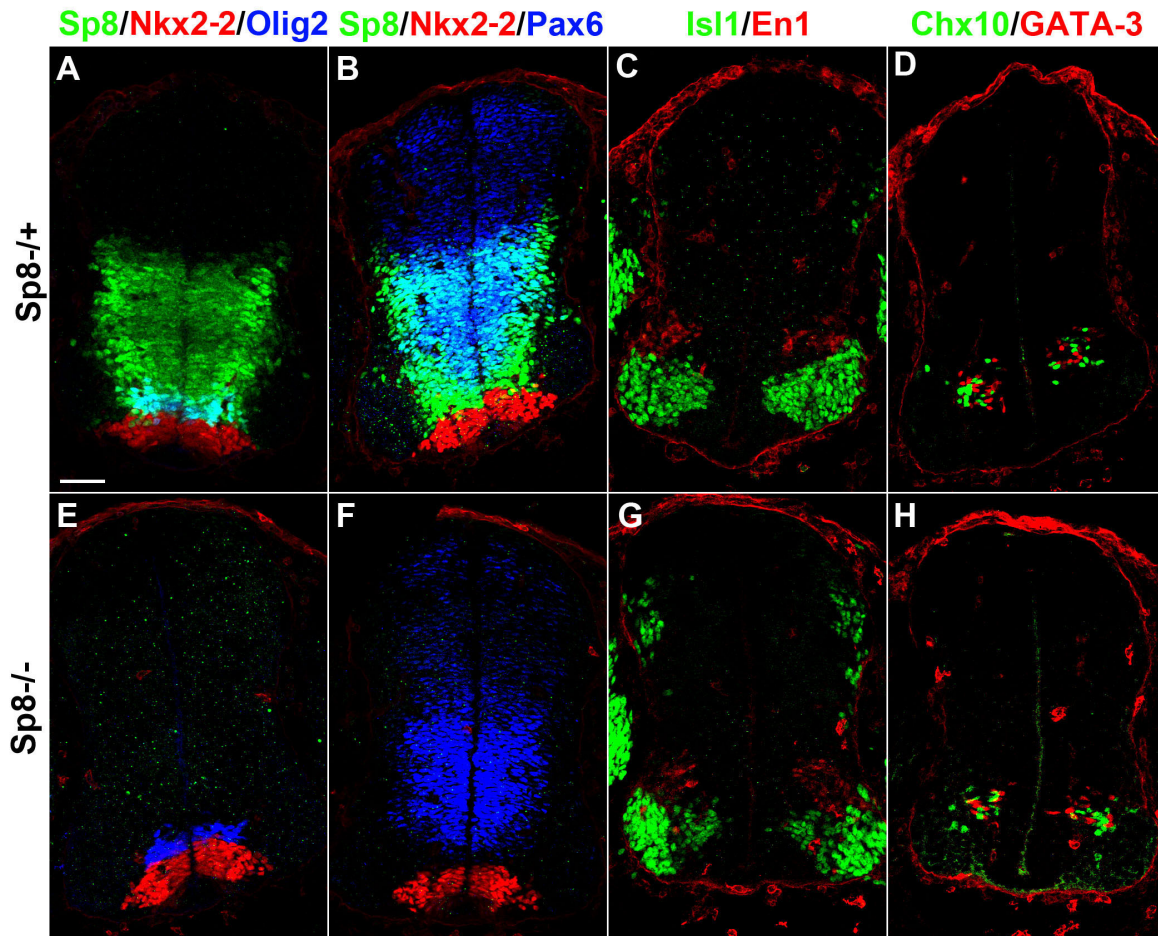


Figure S4. No pattern defects are found in *Sp8* mutant mouse embryos. (A, E) While no *Sp8* expression was detected in the spinal cord of *Sp8*^{-/-} mouse embryos (E) compared to the *Sp8*^{+/-} controls (A), the expression patterns of *Olig2* and *Nkx2-2* were not altered. (B, F) *Pax6* expression was not altered in the *Sp8*^{-/-} embryos (F) compared to the *Sp8*^{+/-} control embryos (B). (C, D, G and H) The generation of *Isl1*⁺ MNs, *En1*⁺ V1 interneurons, *Chx10*⁺ and *GATA-3*⁺ V2 interneurons in the *Sp8*^{-/-} embryos (G,H) was comparable to that in *Sp8*^{+/-} controls (C, D). Scale bar: 50 μ m (shown in A, applies to A-H).

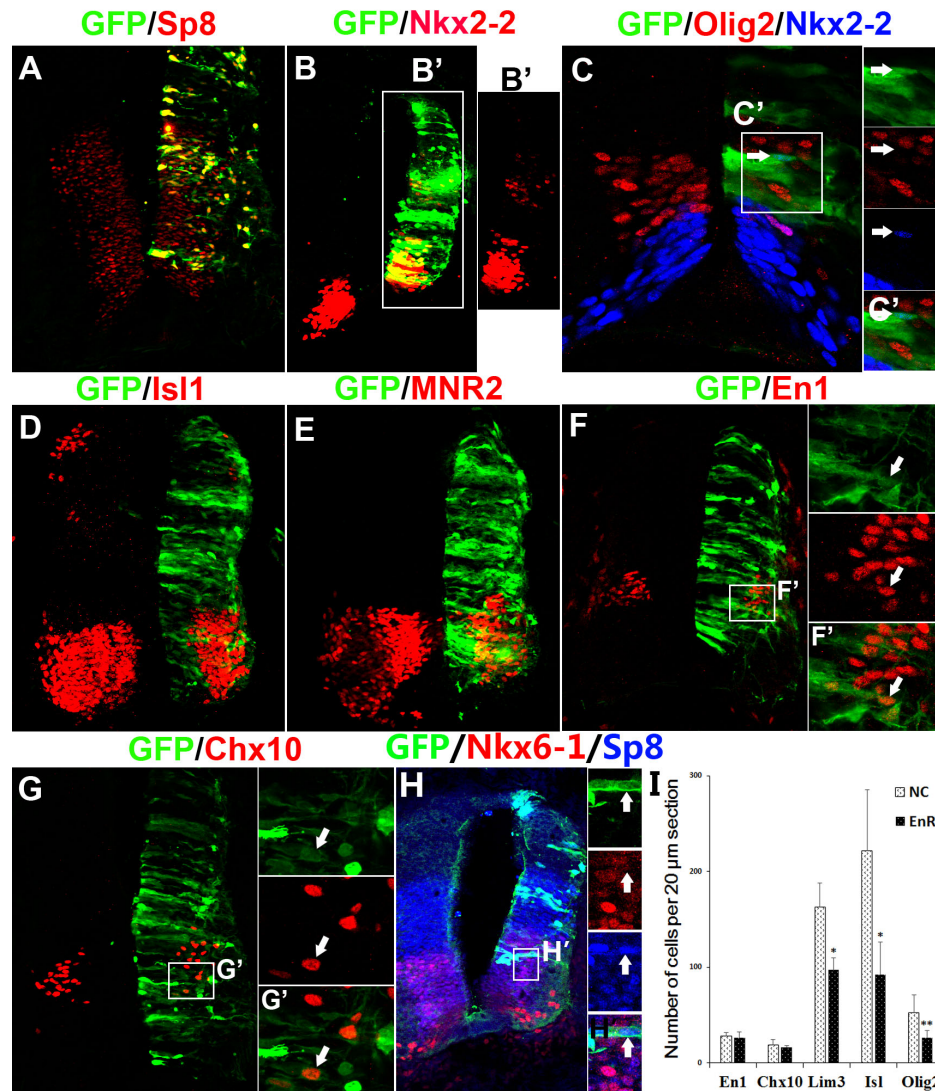


Figure S5. A repressor form of Sp8 (Sp8ZnF::EnR) inhibits MN generation. (A) Nearly all GFP-labeled cells expressed the fusion protein Sp8ZnF::EnR following electroporation. (B, B') The expression of Sp8ZnF::EnR resulted in ectopic Nkx2-2 expression dorsal to the p3 domain in 3/13 embryos (B'). (C, C') Olig2 expression was greatly impaired by Sp8ZnF::EnR expression, but only a subset of Olig2-expressing pMN domain cells exhibited ectopic Nkx2-2 expression (C'). (D, E) The expression of the MN lineage genes Isl1 and MNR2 was reduced following Sp8ZnF::EnR overexpression. (F, G) The overexpression of Sp8ZnF::EnR did not affect the generation of En1+ V1 (arrows in F) or Chx10+ V2 (arrows in G) interneurons. (H) The expression of Sp8ZnF::EnR did not result in ectopic Nkx6-1 expression. Arrows indicate one cell that expressed GFP and Sp8 but not Nkx6-1. (I) Quantification of the above experiments (C-G). Error bars = SEM from 3 chickens per group; * $p < 0.05$; ** $p < 0.01$; Student's t test. Scale bars: 50 μ m (shown in A, applies to A, B, B', D-G); 10 μ m (shown in C, applies to C, C', F', G').

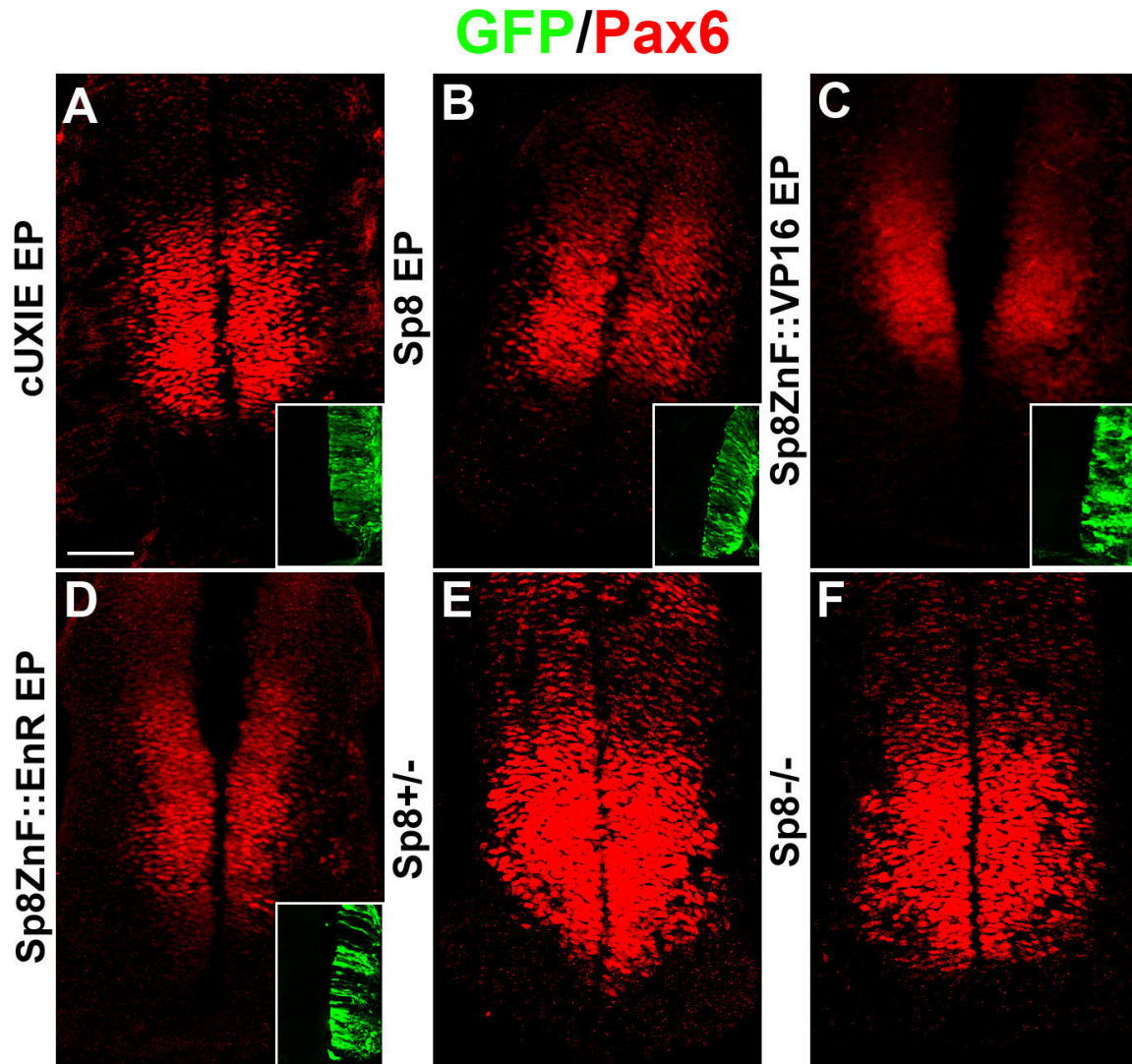


Figure S6. Sp8 does not regulate the expression of Pax6. (A-D) Pax6 expression in the electroporated side was unaffected compared to the unelectroporated control side following electroporation with cUXIE (A), Sp8 (B), Sp8ZnF::VP16 (C) and Sp8ZnF::EnR (D). GFP expression is shown in the insets in (A-D), indicating the expression levels of the exogenous gene. (E, F) The expression pattern of Pax6 in Sp8^{-/-} embryos was very similar to the pattern in the Sp8^{+/-} embryos. Scale bar: 50 μm (shown in A, applies to A-F).

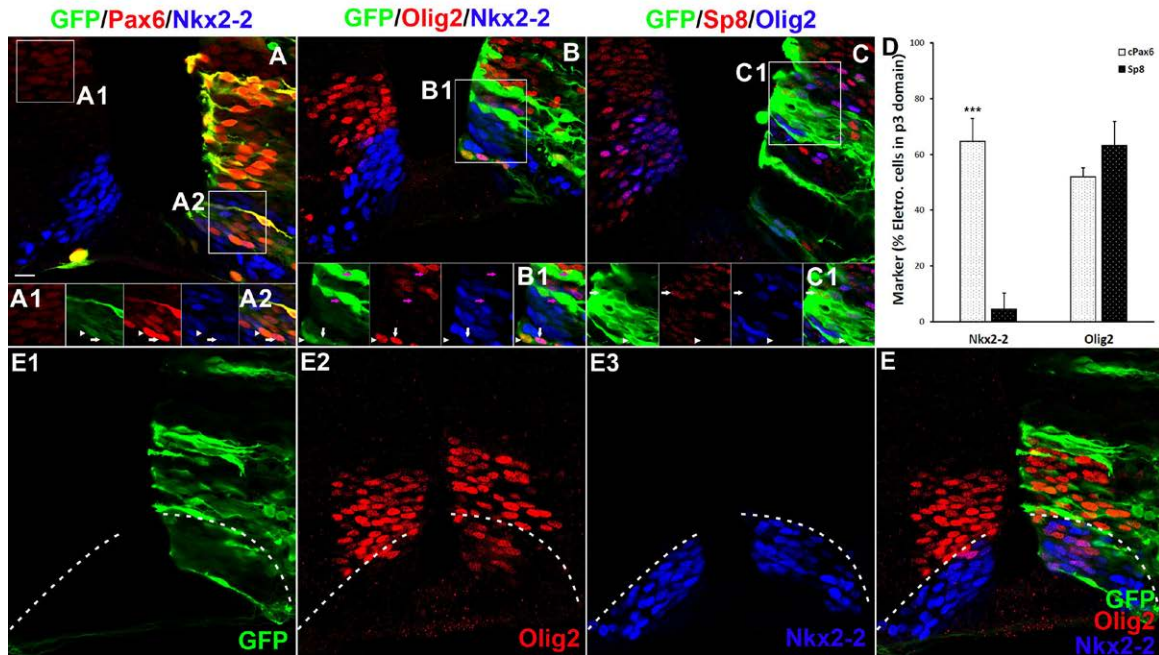


Figure S7. Pax6 misexpression represses Nkx2-2 and induces ectopic Olig2 and Sp8 expression in the p3 domain in a dose-dependent manner. (A-A2) Physiological Pax6 protein levels were defined by the highest Pax6 levels in the unelectroporated side (A1). Pax6 electroporation resulted in the expression of different levels of Pax6 in transfected cells (A2). The expression of Pax6 at much higher than physiological levels extinguished Nkx2-2 expression from p3 progenitors (arrowheads in A2). The cells that expressed physiological levels of Pax6 continued to express lower levels of Nkx2-2 (arrows in A2). (B, B1) One strongly GFP+ cell that expressed Olig2 but not Nkx2-2 (white arrowheads in B1) and one weakly GFP+ cell that expressed both Olig2 and Nkx2-2 (white arrows in B1). The expression of extremely high levels of Pax6 repressed both Olig2 and Nkx2-2 expression in the p3 and pMN domains (magenta arrows in B1). (C, C1) Higher levels of Pax6 repressed both Sp8 and Olig2 expression in the pMN domain (arrowheads in C1). However, Sp8 expression was more commonly observed than Olig2 expression in cells expressing higher levels of Pax6 in the VZ of the pMN domain (arrows in C1). (D) The proportion of the transgenic cells within the p3 domain that expressed Nkx2-2 and Olig2 following cPax6 and Sp8 electroporation. Error bars = SEM from 3 chickens per group; *** $p < 0.001$; Student's t test. (E) The expression of the physiological levels of Pax6 induced Olig2 expression in the p3 domain without abolishing Nkx2-2 expression, resulting in the co-expression of Olig2 and Nkx2-2 in the same cells. Scale bar: 10 μm (shown in A, applies to all images).

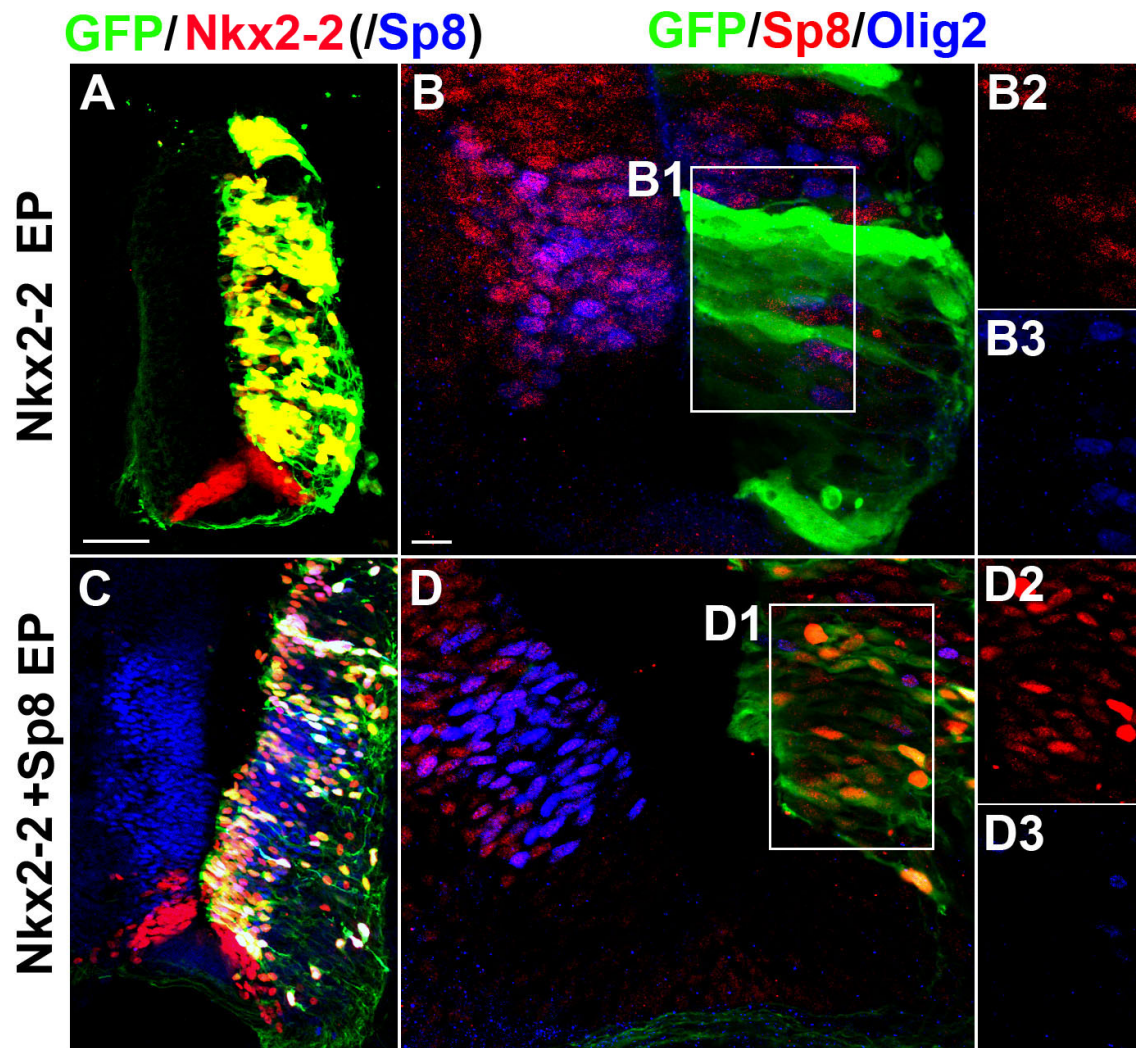


Figure S8. The clearance of Nkx2-2 expression from pMN progenitors is critical for the specification of MN fate. (A) Following Nkx2-2 electroporation, nearly all GFP+ cells expressed Nkx2-2. (B-B3) Nkx2-2 misexpression within the pMN domain inhibited the expression of Olig2. (C) Co-electroporation of Sp8 and Nkx2-2 resulted in 90% GFP-labeled cells co-expressing both Sp8 and Nkx2-2. (D-D3) Sp8 re-expression in pMN progenitors that ectopically expressed Nkx2-2 did not rescue the expression of Olig2. Scale bars: 50 μ m (shown in A, applies to A, C); 10 μ m (shown in B, applies to B-B3, D-D3).

Table S1: List of primary antibodies

Antigen	Host	Dilution	Source	Catalogue #
Pax7	mouse	1/20	DSHB, The University of Iowa (Iowa, USA)	PAX7
MNR2/Hb9	mouse	1/40	DSHB, The University of Iowa (Iowa, USA)	81.5C10
Lhx3/Lim3	mouse	1/30	DSHB, The University of Iowa (Iowa, USA)	67.4E12
En1	mouse	1/20	DSHB, The University of Iowa (Iowa, USA)	4G11
Nkx2-2	mouse	1/40	DSHB, The University of Iowa (Iowa, USA)	74.5A5
Pax6	mouse	1/20	DSHB, The University of Iowa (Iowa, USA)	PAX6
Shh	mouse	1/20	DSHB, The University of Iowa (Iowa, USA)	5E1
FoxA2/Hnf3b	mouse	1/20	DSHB, The University of Iowa (Iowa, USA)	4C7
Islet 1	mouse	1/50	DSHB, The University of Iowa (Iowa, USA)	39.4D5
Chx10	sheep	1/500	Exalpha Biologicals, Inc. (Shirley, MA)	X1179P
Islet 1	rabbit	1/1000	Abcam Inc. (Cambridge, USA)	ab20670
Ki67	rabbit	1/400	Vector Laboratories. (Burlingame, USA)	VP-K451
Mash-1	rabbit	1/1000	Cosmo Bio Co.,Ltd. (Tokyo, Japan)	SK-T01-003
NeuN	mouse	1/400	Chemicon, Millipore. (Temecula, CA)	MAB377
TUJ 1	mouse	1/100	Covance (Princeton, New Jersey)	MMS-435P
Mash-1	mouse	1/100	BD Bioscience (California, USA)	556604
Olig2	rabbit	1/1000	Chemicon, Millipore. (Temecula, CA)	AB9610
Pax6	goat	1/500	Santa Cruz Biotechnology (California, USA)	sc-7750
Pax6	rabbit	1/1000	MBL International Corporation (Woburn, MA)	PD022
GFP	rabbit	1/1000	Aves Labs (Oregon, USA)	GFP-1020
Sp8	goat	1/500	Santa Cruz Biotechnology (California, USA)	sc-104661
GATA-3	mouse	1/200	Santa Cruz Biotechnology. (California, USA)	sc-269
Foxp1	rabbit	1/1000	Abcam Inc. (Cambridge, USA)	ab16645
Nkx6-1	Mouse	1/50	DSHB, The University of Iowa (Iowa, USA)	F55A10